Dark Sectors 2016 Workshop: Community Report

Jim Alexander (VDP Convener),[1] Marco Battaglieri (DMA Convener),[2] Bertrand Echenard (RDS Convener),[3] Rouven Essig (Organizer),[4,*] Matthew Graham (Organizer),[5,†] Eder Izaguirre (DMA Convener),[6] John Jaros (Organizer),[5,‡] Gordan Krnjaic (DMA Convener),[7] Jeremy Mardon (DD Convener),[8] David Morrissey (RDS Convener),[9] Tim Nelson (Organizer),[5,§] Maxim Perelstein (VDP Convener),[1] Matt Pyle (DD Convener),[10] Adam Ritz (DMA Convener),[11] Philip Schuster (Organizer),[5,6,¶] Brian Shuve (RDS Convener),[5] Natalia Toro (Organizer),[5,6,**] Richard G Van De Water (DMA Convener),[12] Daniel Akerib,[5,13] Haipeng An,[3] Keith Baker,[14] Dipanwita Banerjee,[15] James Beacham,[16] Nikita Blinov,[5] Mariangela Bondí,[17] Walter Bonivento,[5] Stan Brodsky,[5] Ran Budnik,[18] Massimo Carpinelli,[19,20] Concetta Cartaro,[5] David Cassel,[21,5] Gianluca Cavoto,[22] Andrea Celentano,[23] Animesh Chaterjee,[24] Saptarshi Chaudhuri,[8] Gabriele Chiodini,[25] Hsiao-Mei Sherry Cho,[5] Robert Cooper,[26] Ross Corliss,[27] Marzio De Napoli,[17] Raffaella De Vita,[23] Achim Denig,[28] Ranjan Dharmapalan,[29] Bogdan Dobrescu,[30] Raphael Dupre,[31] Juan Estrada,[7] Clive Field,[5] Bartosz Fornal,[32] Alexander Friedland,[5] Iftach Galon,[32] Susan Gardner,[33,34] Andrey Golutvin,[35,36] Stefania Gori,[37] Enrico Graziani,[38] Keith Griffioen,[39] Keith Griffioen,[39] Andrew Haas,[40] Keisuke Harigaya,[10,41] Christopher Hearty,[42] Scott Hertel,[10,41] JoAnne Hewett,[5] David Hitlin,[3] Maurik Holtrop,[43] Lauren Hsu,[30] Kent Irwin,[5] Igal Jaegle,[44] Yonatan Kahn,[45] Noah Kurinsky,[5,8] Ranjan Laha,[13,8] Gaia Lanfranchi,[46] Dale Li,[5] Tongyan Lin,[10,41] Kun Liu,[12] Ming Liu,[12] Dinesh Loomba,[47] Aaron Manalaysay,[48] Jeremiah Mans,[49] Thomas Markiewicz,[5] Takashi Maruyama,[5] Dan McKinsey,[10] Jeremy Mock,[50] Maria Elena Monzani,[5] Corina Nantais,[51] Sebouh Paul,[51] Michael Peskin,[5] Antonio D Polosa,[52,53] Maxim Pospelov,[6,54] Igor Rachek,[55] Mauro Raggi,[22] Nunzio Randazzo,[17] Blair Ratcliff,[5] Thomas Rizzo,[5] Dylan Rueter,[8] Ani Simonyan,[56] Valeria Sipala,[19,20] Elton Smith,[57] Daniel Snowden-Ifft,[58] Matthew Solt,[5] James Spencer,[5] Stepan Stepanyan,[57] Michael Sullivan,[5] Flip Tanedo,[32] Rex Tayloe,[59] Jesse Thaler,[27] Sho Uemura,[5] Holly Vance,[60] Jerry Vavra,[5] Mike Williams,[27] Bogdan Wojtsekhowski,[57] Jong Min Yoon,[5,8] Hai-Bo Yu,[61] Tien-Tien Yu,[4] Yue Zhang,[3] Yue Zhao,[62] Yiming Zhong,[4] and Kathryn Zurek[41,10]

[1] *LEPP, Cornell University, Ithaca, NY 14853, USA*
[2] *INFN*
[3] *California Institute of Technology, Pasadena, California 91125, USA*
[4] *C.N. Yang Institute for Theoretical Physics, Stony Brook University, Stony Brook, NY 11794-3800*
[5] *SLAC National Accelerator Laboratory, Menlo Park, CA 94025, USA*
[6] *Perimeter Institute for Theoretical Physics, Waterloo ON N2L 2Y5, Canada*
[7] *Fermilab*
[8] *Stanford University Physics Department, Stanford, CA 94305, USA*
[9] *TRIUMF, Vancouver, BC V6T 2A3, Canada*
[10] *Department of Physics, University of California, Berkeley, California 94720, USA*
[11] *University of Victoria*
[12] *Los Alamos National Lab*
[13] *KIPAC*
[14] *Yale University*
[15] *Institute for Particle Physics, ETH Zurich, 8093 Zurich, Switzerland*

[16]Ohio State University
[17]Istituto Nazionale di Fisica Nucleare, Sezione di Catania, 92125 Catania, Italy
[18]Weizmann Institute of Science
[19]Istituto Nazionale di Fisica Nucleare, Laboratori Nazionali del Sud, 92125 Catania , Italy
[20]Università di Sassari, 07100 Sassari, Italy
[21]Cornell
[22]Istituto Nazionale di Fisica Nucleare, Sezione di Roma, 00185 Roma, Italy
[23]Istituto Nazionale di Fisica Nucleare, Sezione di Genova, 16146 Genova , Italy
[24]University of Texas at Arlington
[25]Istituto Nazionale di Fisica Nucleare, Sezione di Lecce, 73047, Italy
[26]New Mexico State University
[27]Massachusetts Institute of Technology, Cambridge, MA 02139, USA
[28]JGU Mainz, Institute for Nuclear Physics
[29]Argonne National Laboratory, Lemont, IL 60439, USA
[30]Fermi National Accelerator Laboratory
[31]Institut de Physique Nucléaire, CNRS-IN2P3, Univ. Paris-Sud, Université Paris-Saclay, 91406 Orsay Cedex, France
[32]Department of Physics and Astronomy, University of California, Irvine, California 92697, USA
[33]University of Kentucky
[34]UCI
[35]Imperial College
[36]CERN
[37]University of Cincinnati
[38]Istituto Nazionale di Fisica Nucleare, Sezione di Roma Tre, 00146 Roma, Italy
[39]College of William and Mary
[40]NYU
[41]Lawrence Berkeley National Laboratory, Berkeley, California 94720, USA
[42]University of British Columbia
[43]University of New Hampshire
[44]University of Hawaii
[45]Princeton University
[46]Istituto Nazionale di Fisica Nucleare, Laboratori Nazionali di Frascati, 00044 Frascati, Italy
[47]University of New Mexico
[48]University of California, Davis
[49]University of Minnesota
[50]University at Albany
[51]College Of William And Mary
[52]CERN Theory Department, CH-1211 Geneva 23, Switzerland
[53]Università di Roma La Sapienza, 00185 Roma, Italy
[54]Victoria
[55]Budker Institute of Nuclear Physics
[56]IPNO
[57]Jefferson Laboratory, Newport News, VA 23606, USA
[58]Occidental College
[59]Indiana University Center for Exploration of Energy and Matter
[60]Old Dominion University

[61] *University of California, Riverside*
[62] *University of Michigan*
(Dated: August 11, 2016)

*Electronic address: rouven.essig@stonybrook.edu
†Electronic address: mgraham@slac.stanford.edu
‡Electronic address: john@slac.stanford.edu
§Electronic address: tknelson@slac.stanford.edu
¶Electronic address: schuster@slac.stanford.edu
**Electronic address: ntoro@slac.stanford.edu

Contents

I. EXECUTIVE SUMMARY

This report, based on the Dark Sectors workshop at SLAC in April 2016, summarizes the scientific importance of searches for dark sectors, the status of this growing international field, the important milestones motivating future exploration, and the experimental opportunities to reach these milestones.

Remarkably, 80% of the matter in the Universe is an unknown substance — Dark Matter — whose constituents and interactions are quite different from those of ordinary matter. The 2014 P5 report highlights the vital importance of identifying the physics of Dark Matter and of making this search as broad as possible — particularly given the absence of evidence for WIMPs at the LHC and direct detection experiments. A simple possibility is that dark matter interacts through a new force that is similar in structure to known forces but couples only indirectly to ordinary matter. While particle physics has traditionally focused on exploring matter at ever-smaller scales through high-energy experiments, testing this dark-sector hypothesis requires innovative low energy experiments that use high-intensity beams and/or high-sensitivity detectors.

Since 2009, several hundred physicists at over a dozen experiments have mined a wealth of existing data and proven new techniques to search for dark-sector physics, focused primarily on the possible signal of a new force carrier that decays into pairs of charged particles. In parallel, recent experimental and theoretical work has shown the importance, feasibility, and complementarity of searching for dark sectors by hunting the Dark Matter itself.

Building on this progress, proposed dark sector experiments over the next decade aim to decisively explore simple sub-GeV dark sectors, and cover as much ground as possible for higher-mass or richer dark sectors, by

- Extending the search for visibly decaying force carriers to higher masses and, for force-carriers lighter than about half the proton mass, fully exploring the range of mixing parameter that can arise from simple quantum effects
- Extending searches for light dark matter production at accelerators, ultimately probing the minimum Dark Matter coupling required for simple models of sub-GeV thermal dark matter, and
- Extending Dark Matter direct detection searches to lower energy thresholds, to test models of thermal and freeze-in Dark Matter and eventually probe the warm Dark Matter mass limit of 1 keV

These three goals are complementary, and to explore the physics of dark sectors we must pursue them in parallel. Together, they guide the Dark Sectors program in the US and abroad. A robust dark-sector program entails parallel investment in several small-scale experiments, support for facilities that can enable these experiments, and judicious use of existing multi-purpose detectors. The discovery of a dark sector would not only shed light on the mystery of Dark Matter but also open a window on a whole new sector of the Universe.

The best ideas of the community for exploring and revealing this new physics are summarized in this report.

II. INTRODUCTION

A. Scientific Context and Goals

Elementary particle physics seeks to discover and understand the most basic constituents of Nature. Our current knowledge is encompassed in the Standard Model (SM) of particle physics. While the SM is phenomenally successful in describing the physics of familiar matter to high precision, in a wide variety of environments and over a large energy range, it is also known to be incomplete. In particular, new physics must be responsible for the Dark Matter, for neutrino masses, and for the matter-antimatter asymmetry in Nature.

The hunt for physics beyond the Standard Model encompasses several distinct directions. One of these directions is the search for a *dark sector*, which we define to be a collection of particles that are not charged directly under the SM strong, weak, or electromagnetic forces. Such particles are assumed to possess gravitational interactions, and may also interact with familiar matter through several "portal" interactions that are constrained by the symmetries of the Standard Model.

The exciting possibility of a dark sector is motivated in part by the ease with which dark sectors can explain the known gaps in the Standard Model (dark matter, neutrino masses, and a baryon asymmetry). The only well-established features of Dark Matter are its lack of strong or electromagnetic interactions and its abundance. A dark sector is a very natural scenario to explain this paucity of interactions, and can readily produce the observed Dark Matter abundance through thermal freeze-out or freeze-in, as discussed below. Likewise, sterile neutrinos — a very simple dark sector — are the canonical hypothesis for the origin of neutrino masses. The interactions of either sterile neutrinos or a more complex dark sector can readily introduce the ingredients needed to produce a matter-antimatter asymmetry and transmit it to the baryon sector. A non-trivial dark sector, with new interactions beyond the Standard Model's, could leave an imprint on other physics in several ways: self-interactions of dark matter may affect the dynamics of galactic structure formation, and portal interactions can affect precision measurements such as the anomalous magnetic moment of the muon and the proton charge radius; indeed, discrepancies between simulation/theory and experiment in all of these measurements have been suggested as possible hints of a dark sector [].

More broadly, the possibility of a dark sector is a generic one, with significant implications for our understanding of the Universe, yet poorly tested. The indirect nature of a dark sector's interactions with ordinary matter means that it could easily evade detection in the sequence of experiments that has guided particle physics in its exploration of increasingly higher-energy physics — even if the particles of the dark sector are relatively light. Rather, finding and studying a dark sector requires dedicated searches at high precision and/or intensity. Even though the definition of a dark sector is extremely broad, its physics can be explored effectively and systematically by using the specific portal interactions as a guide.

It is natural and pragmatic that the greatest focus in the search for dark sectors has been on the mass range where these high-intensity searches are most feasible (and where conventional searches are least effective), from MeV masses to a few GeV. This range (and above) is also a parameter region of great interest for dark-sector DM, where the portal interaction can guarantee thermal equilibrium between the DM and ordinary matter in the early Universe; dark sectors in this mass range are also particularly relevant to several of the experimental/observational anomalies noted above. Within this parameter space, there are several natural targets, discussed in §**??**, which serve as milestones against which dark-sector

experiments can be judged.

The last decade has seen tremendous progress in the search for MeV-to-GeV mass dark states. Naturally, the bulk of early results have come from theoretical studies and reanalyses of existing datasets from experiments designed for other purposes. A growing sequence of dedicated experiments are presently collecting data [1**?** **?**] and in some cases already publishing physics results [**?** **?** **?**]. There is now a tremendous opportunity for rapid progress and new discoveries in this area, with several new and timely proposals to pursue the most important and well-motivated dark-sector targets with new or existing colliding-beam, fixed-target, and direct-detection experiments. A program of experiments, built with the goal of achieving the milestones articulate in this document, has a tremendous potential to revolutionize particle physics through a discovery of a dark sector. Even if no discovery is made, this program will still have a significant and lasting impact by dramatically narrowing the range of viable Dark Matter candidates and dark sector scenarios.

1. Dark Sectors 2016 Workshop

This report summarizes recent developments, important scientific milestones, experimental opportunities, and provides an updated discussion of dark sector theory. The contents are based on the findings of the Dark Sectors 2016 workshop, held at the SLAC National Accelerator Laboratory in April 2016. The workshop had several plenary sessions and four working groups: Dark Matter at Accelerators (DMA), "Visible" Dark Photons (VDP), Rich Dark Sectors (RDS), and Direct Detection (DD). Our report is structured in the same way with identical section titles. Each working group had both experimentalist and theorist conveners who coordinated the presentations and discussions. A closeout session presented the findings and recommendations of the working groups. The sections in this report have been assembled by the conveners, and they are designed to reflect the contents and findings of each working group and closeout. While this report serves in part as a summary of the current status of the field (see [10–12] for recent reviews), the purpose of Dark Sectors 2016 was to discuss the scientific goals of the field, and the best ideas for new experiments that can achieve these goals. No decisive attempt was made to prioritize one experimental approach over another, as many approaches are still in research and development phases, but relative strengths and weaknesses were identified and have been articulated in this report.

We focus largely on searches for dark photons, decaying either to SM or dark-sector particles, and searches for dark matter coupled to dark photons. This allows for a comprehensive survey of the wide-ranging phenomenology present in this scenario, and is sufficient to demonstrate the salient features of the most important experimental approaches that are needed. We additionally comment on the theoretical motivations and experimental prospects for more general dark sectors beyond the vector portal. We will not review in detail developments in searches for axions or axion-like particles, milli-charged particles, or ATLAS and CMS searches for dark sectors, although some of these experiments are discussed in the context or rich dark sectors.

Below, we summarize the key interactions that dark sector experiments can probe, guided by fundamental symmetries of the Standard Model. We then describe important theoretical targets in parameter space that serve as concrete goals for the next generation of experiments. We then discuss the complementary of different approaches, emphasizing what is already well known when searching for weak-scale physics: only a comprehensive and multi-faceted approach can probe the range of dark-sector possibilities. The working group summary

sections follow.

2. *The "Portal" Interactions*

Dark sectors typically connect via a *portal* to the SM through one or more mediator particles. The portal relevant for dark sector-SM interactions depends on the mediator spin and parity: it can be a scalar ϕ, a pseudoscalar a, a fermion N, or a vector A'. The gauge and Lorentz symmetries of the SM greatly restrict the ways in which the mediator can couple to the SM. The dominant interactions between the SM and these mediators are the following SM gauge singlet operators:

$$\mathcal{L} \supset \begin{cases} -\dfrac{\epsilon}{2\cos\theta_W} B_{\mu\nu} F'^{\mu\nu} \,, & \text{vector portal} \\ (\mu\phi + \lambda\phi^2) H^\dagger H \,, & \text{Higgs portal} \\ y_n L H N \,, & \text{neutrino portal} \\ \frac{a}{f_a} F_{\mu\nu} \widetilde{F}^{\mu\nu} \,, \ \ldots \,, & \text{axion portal.} \end{cases} \tag{1}$$

Here, H is the SM Higgs doublet with charge assignment $(1, 2, +\frac{1}{2})$ under the SM gauge group $SU(3)_c \times SU(2)_L \times U(1)_Y$, L is a lepton doublet of any generation transforming as $(1, 2, -\frac{1}{2})$, $B_{\mu\nu} \equiv \partial_\mu B_\nu - \partial_\nu B_\mu$ is the hypercharge field strength tensor, $F_{\mu\nu}$ ($\widetilde{F}_{\mu\nu}$) is the (dual) field-strength tensor of the SM photon field, θ_W is the weak mixing angle, and $F'_{\mu\nu} \equiv \partial_\mu A'_\nu - \partial_\nu A'_\mu$ is the field strength of a dark $U(1)_D$. The first three operators are renormalizable (dimension-4), while the axion portal is dimension-5 and suppressed by some (high) mass scale. These four portals are arguably the most important ones to consider when discussing dark sectors.

Our focus will be on the vector portal, but we briefly comment on the other portals. If the mediator is a scalar, it can interact via the Higgs portal. This is probed in various ways, including exotic Higgs decays at high-energy colliders such as the LHC [RE: cites?]. If we require the scalar ϕ to be sub-GeV, then various constraints already exist [2, 3] [RE: others?]. Fermionic mediators N play the role of a right handed neutrino with a Yukawa coupling y_ν. N can itself be a viable, cosmologically metastable (non-thermal) DM candidate in a narrow mass range, $m_N \sim$ keV [4]. For m_N in the MeV-to-GeV range, there are strong constraints from beam dumps, rare meson decays, and Big Bang Nucleosynthesis [5]. For pseudoscalar mediators, an extensive literature exists, see e.g. [6] and references therein.

We focus on the vector portal, as it is the most viable for thermal models of light DM (LDM). If the mediator is a vector boson from an additional $U(1)_D$ gauge group under which LDM is charged, the "kinetic mixing" interaction $\epsilon/\cos\theta_W B^{\mu\nu} F'_{\mu\nu}$ is gauge invariant under both $U(1)_D$ and $U(1)_Y$. Here ϵ is, *a priori* a free parameter, though it often arises from loops of heavy states charged under both groups are integrated out at a high scale, so it is generically expected to be small, $\epsilon \sim 10^{-3}$ or smaller [7]. Additionally, its phenomenology is representative of a broader class of well-motivated models, such as the scenarios where the mediator couples preferentially to baryonic, or leptonic, or $(B - L)$ currents, respectively. Finally, simple models of the vector portal admit various couplings of DM to the $U(1)_D$ gauge boson. The DM could, for example, have Majorana couplings to the mediator that affect the phenomenology (see [8] for an example), or it could live in a rich sector (*e.g.*, see [9]).

B. Important Milestones

To discuss important vector-portal dark milestones, we introduce a simple and minimal dark sector model. This model can easily be expanded to describe more complicated theories.

1. Models

A starting point for our discussion is the **minimal kinetically mixed dark photon**, a vector field A'^{μ} with Lagrangian

$$\mathcal{L}_{\mathrm{A}'} = -\frac{1}{4}F'^{\mu\nu}F'_{\mu\nu} + \frac{1}{2}\frac{\epsilon}{\cos\theta_W}B^{\mu\nu}F'_{\mu\nu} - \frac{1}{2}m^2_{A'}A'^{\mu}A'_{\mu} \tag{2}$$

where $F'_{\mu\nu} \equiv \partial_\mu A'_\nu - \partial_\nu A'_\mu$ is the dark photon field strength and $B_{\mu\nu} \equiv \partial_\mu B_\nu - \partial_\nu B_\mu$ is the Standard Model hypercharge field strength. This model, parameterized by the dark photon mass $m_{A'}$ and kinetic mixing parameter ϵ, comprises one of the simplest possible dark sectors in its own right, and it can also represent the mediator portion of a larger dark sector. For MeV–GeV-mass dark photons, the dominant effect of this kinetic mixing, after electroweak symmetry breaking, is an analogous mixing $\frac{1}{2}\epsilon F'_{\mu\nu}F^{\mu\nu}$ with the Standard Model electromagnetic field strength $F^{\mu\nu}$, where $\epsilon = \epsilon_Y \cos\theta_W$. In the basis with diagonal and canonically normalized kinetic terms, the result of the kinetic mixing is that the dark photon acquires a coupling of strength $e\epsilon$ to the electromagnetic current.

Since the DM puzzle is among the main motivations for a dark sector, it is natural to extend this minimal model by a DM candidate. This DM can be a fermion or a scalar boson that couples to the dark photon through dark-sector gauge interactions

$$\mathcal{L}_{DM(f)} = \bar{\chi}(i\not{D} - m_\chi)\chi, \quad \text{or} \tag{3}$$

$$\mathcal{L}_{DM(s)} = (D^\mu\phi)^*(D_\mu\phi) - m^2_\phi|\phi|^2, \tag{4}$$

where $D_\mu \equiv (\partial_\mu - ig_D A_\mu)$ and g_D is the dark-sector coupling. The dark photon mediates interactions between DM and the SM electromagnetic current that motivates various laboratory experiments. Because the A' is massive, the dark gauge symmetry may be spontaneously broken by a dark Higgs boson. In this case, Majorana mass terms may also be allowed,

$$\Delta\mathcal{L}_{DM(f)} = -\frac{\delta}{2}\bar{\chi}^c\chi + \text{h.c.}, \quad \text{or} \tag{5}$$

$$\Delta\mathcal{L}_{DM(s)} = -\frac{\delta^2}{2}\phi\phi + \text{h.c.} \tag{6}$$

Because these mass terms must vanish with the restoration of the gauge symmetry, they are naturally small (δ naturally $\ll m_\chi$). The effect of such "inelastic splittings" on dark matter phenomenology is significant — they split a Dirac dark matter fermion into two Majorana states (or a complex scalar into two real ones), and the leading dark gauge interaction mediates a transition from the light state to the heavier one, or vice versa [13]. This significantly alters constraints from DM direct and indirect detection and modifies the DM targets for various experiments. [RE: discuss]

2. Targets in Parameter Space

While the model above has a broad parameter space, several specific regions are particularly important targets – either because they are theoretically well-motivated, or because exploring these regions decisively tests outstanding anomalies (*e.g.*, $(g-2)_\mu$ [14]), or because they represent a challenging new experimental frontier. We will now present concrete experimental targets. We emphasize, however, that any experiment should try not only to probe these targets, but go well beyond them, as often simple changes in a model can alter the target parameter space.

- **Thermal DM freeze-out**: Thermal freeze-out of Dark Matter (DM) annihilations into ordinary matter is a simple and predictive explanation for the origin of the DM abundance measured today. It is the basis for the "WIMP Miracle" in TeV-scale weakly interacting DM models but applies equally to dark sector DM, and predicts a thermally-averaged DM annihilation cross-section of $\approx 3\times10^{-26}\text{cm}^3/\text{s}$ with only mild dependence on the DM mass.

  For all mediators and LDM candidates χ, there is a basic distinction between "secluded" annihilation to pairs of mediators (via $\chi\chi \to$ A' A' for $m_\chi > m_{A'}$) followed by mediator decays to SM particles [17], and "direct" annihilation to SM final states (via virtual mediator exchange in the s-channel, $\chi\chi \to \text{A}'^* \to$ SM SM for $m_\chi < m_{A'}$) without an intermediate step.

  For the secluded process, the annihilation rate scales as

  $$(\text{"secluded" annihilation}) \qquad \langle\sigma v\rangle \sim \frac{g_D^4}{m_\chi^2} \quad , \tag{7}$$

  where g_{DM} is the coupling between the mediator and the LDM, and there is no dependence on the SM-mediator coupling g_{SM}. Since arbitrarily small values of g_{SM} can be compatible with thermal LDM in this regime, the secluded scenario does not lend itself to decisive laboratory tests. For secluded annihilations to be kinematically allowed, $m_{A'} < m_\chi$, which is suggestive of visible dark photon decays.

  The situation is markedly different for the direct annihilation regime in which $m_\chi < m_{A'}$ where the annihilation rate scales as

  $$(\text{"direct" annihilation}) \qquad \langle\sigma v\rangle \sim \frac{g_D^2\, g_{\text{SM}}^2\, m_\chi^2}{m_{A'}^4} \quad , \qquad , \tag{8}$$

  and offers a clear, predictive target for discovery or falsifiability, since the dark coupling g_D and mass ratio $m_\chi/m_{A'}$ are at most $\mathcal{O}(1)$ in this $m_{A'} > m_\chi$ regime, so there is a minimum SM-mediator coupling compatible with a thermal history; larger values of g_D require nonperturbative dynamics in the mediator-SM coupling or intricate model building. This mixing target, at the level of $\epsilon \sim 10^{-7} m_{A'}^2/(m_\chi\,\text{MeV}\sqrt{\alpha_D})$, is an important benchmark for both dark photon and dark matter searches.

- **Freeze-in**: An alternative to the thermal DM scenario is one where the DM abundance is established via "freeze-in" [18]. In freeze-in scenarios, the dark sector is never in thermal equilibrium with the SM, but out-of-equilibrium scattering gradually populates the DM. Because thermal equilibrium is not established between the dark and visible sectors, the couplings in freeze-in scenarios are typically very small.

Consider a simple example with a kinetically mixed dark photon, A', which can decay to two DM particles, χ. The dark photon is gradually produced through out-of-equilibrium scatterings, and the dark photons then decay to establish the DM abundance. To obtain the observed DM abundance, the couplings must satisfy [18]

$$\frac{\epsilon^2 m_\chi}{m_{A'}} \sim 10^{-26}\, g_*^{3/2}, \tag{9}$$

where g_* is the number of degrees of freedom in the SM plasma at the $T \sim m_{A'}$.

A variation of this model is to take $m_{A'}$ to be tiny $\ll$eV. In this case, the DM abundance is also built up slowly over time through SM particles annihilating to DM particles through an off-shell A'. Here the final DM abundance is independent of $m_{A'}$, and there is only a mild dependence on m_χ above ~ 1 MeV. For example, for $m_\chi = 100$ MeV, the couplings needed to obtain the correct relic abundance are given by [19, 20]

$$\alpha_D \epsilon^2 \sim 3 \times 10^{-24}\,. \tag{10}$$

Such small couplings are impossible to probe at colliders or fixed-target experiments, but novel low-threshold direct detection techniques have an opportunity to probe them in the near future.

Freeze-in thus motivates an entirely complementary set of parameters from thermal scenarios, and any experiment that is sensitive to very tiny couplings can test DM from freeze-in.

- **The 2-loop region for Kinetic Mixing ($\epsilon \gtrsim 10^{-6}$), from MeV to $\sim$ GeV energies:** While the strength of kinetic mixing ϵ is arbitrary, certain ranges of coupling are motivated because they readily arise from the quantum effects of heavier particles. In particular, loops of a heavy particle that carries both hypercharge and $U(1)_D$ charge typically generate $\epsilon \sim 10^{-2} - 10^{-4}$ [7]. Moreover, the particle content and gauge couplings of the SM raise suggestive hints that, at high energies, hypercharge may be unified with other SM gauge forces into a larger non-Abelian gauge symmetry (i.e. a Grand Unified Theory or GUT) [15]. In this case, the enhanced symmetry of the GUT guarantees that ϵ must vanish at tree-level and that the one-loop contributions to ϵ from heavy particles also vanish. In fact, the leading contribution to ϵ arises at two-loop order, with characteristic size $\epsilon \sim 10^{-3} - 10^{-6}$ [16].

  Fully exploring the range of kinetic mixing strength that can arise from 1- or 2-loop effects is therefore an important milestone for dark-sector searches (although it should be noted that much smaller ϵ are also compatible with GUTs, and can arise for example if the mixing is non-perturbative or arises at 3-loop level). At present, there are plausible strategies to explore the full 2-loop mixing parameter space only for dark photon masses $\lesssim 1$ GeV — but this upper mass limit is imposed simply by experimental feasibility, not theoretical motivation.

- **Direct Dark Photon Searches above a GeV**: Searches for dark photons above 1 GeV in mass are more challenging for several reasons — these dark photons have lower production cross-sections and (in the case of visible decays) shorter decay lengths for a given ϵ. As such, while dedicated fixed-target experiments have a crucial role to play in low-mass dark sector searches, the range $m_{A'} \gtrsim 1$ GeV is best explored through

searches at multi-purpose colliders — including high-luminosity B-factories (Belle-II) and high-energy pp collider experiments (ATLAS, CMS and LHCb) [RE: need to give citations]. Given the unique mass reach of these experiments, it is essential to develop techniques and upgrades that can improve their sensitivity to dark sectors and exploit them fully (e.g. mono-photon trigger).

- **Direct-detection down to the warm DM mass limit of ∼keV** In general, DM that is in thermal equilibrium with ordinary matter in the early Universe can decouple while it is relativistic if its mass is low enough. DM that remains relativistic until after matter-radiation equality (i.e. for temperatures $\lesssim 1$ eV), so-called "hot" DM, is well excluded by cosmological observations. However, even if DM is heavier and becomes non-relativistic before matter-radiation equality, it can still wash out small-scale structure. The current lower bound is about 1 keV, and comes from Lyman-α forest measurements [RE: be more precise, cite]. Dark matter above this mass is consistent with the known structure formation history of the Universe. Therefore, reaching the keV-mass threshold (with, for example, direct-detection experiments) presents an interesting, if challenging, target.

- **Closing the partially visible muon $g-2$ region**: The anomalous magnetic dipole moment of the muon, $(g-2)_\mu$, is a property of the muon that is precisely measured and is more sensitive than $(g-2)_e$ to new interactions in the GeV range. There is a long-standing discrepancy between the SM prediction for $(g-2)_\mu$ and its experimentally measured value [21, 22]. While improved theoretical calculations and experimental precision should shed light on this discrepancy in the future, it is worth investigating how models of new physics can account for the anomaly. In particular, dark sector states such as dark photons can account for the anomaly with $\epsilon \gtrsim 10^{-3}$ [14]. The $(g-2)_\mu$ discrepancy provides a concrete target that can be probed by dark-sector experiments.

  In the simplest example of a visibly decaying, kinetically mixed dark photon, the entire $(g-2)_\mu$ preferred region is now excluded [23]. However, a dark photon can decay predominantly into dark-sector states, in which case there is still a region of parameter space that accounts for $(g-2)_\mu$ and is compatible with other experiments. For example, if A' decays invisibly, or decays partially visibly ($A' \to \chi_2\chi_1$, $\chi_2 \to \chi_1$+SM for invisible χ_1) as in models of inelastic DM, then A' can explain the $(g-2)_\mu$ discrepancy. Also, since most constraints on the $(g-2)_\mu$ assume interactions of A' with light-flavor quarks and leptons, a model that couples A' predominantly to heavy-flavor leptons can evade the $(g-2)_\mu$ constraints.

C. Complementarity Between Experimental Approaches

The above discussion shows that, even in a relatively minimal model of DM with a dark photon, a range of distinct phenomenology is expected. An experimental program to test GeV-scale hidden sectors should therefore encompass a range of signatures. In this section, we comment on a few cases in which different experiments probe dark sectors in complementary ways, with many more details provided in the body of the report.

In the well-motivated scenario of an invisibly decaying mediator, there are two main approaches to observing a dark-sector signature: either a detector is placed downstream

from the A' production at a beam dump and scattering between the invisible states and detector material is observed, or the presence of the invisible states is inferred from missing momentum (either at a high-energy collider or fixed-target experiment). The strength of missing momentum techniques is that sensitivity scales with production cross section, and no additional penalty need to payed to re-scatter states downstream. The technique is also largely independent of the dark sector coupling so long as little or no visible decays are recorded. The strength of beam dump experiments is that the invisible states themselves are detected.

There also exists complementarity between direct detection experiments and accelerator-based probes. In the MeV-GeVmass range, both direct detection and accelerator based techniques can probe elastic scattering DM scenarios, but only accelerator based experiments are able to broadly explore scenarios such as inelastic DM. Beam-dump and missing-momentum experiments are also readily capable of probing meta-stable states unrelated to DM, or any sub-dominant DM components. On the other hand, the prospects for direct detection look better than for accelerator techniques in the case of ultra low-mass (sub-keV) mediators, where the elastic cross section is enhanced by the small momentum transfer in scattering. If the A' itself is the DM, direct detection experiments can have excellent sensitivity to DM absorption (similarly, scalars or pseudoscalars can have such absorption signal). Perhaps most exciting, there are several scenarios discussed above in which different experimental approaches can see a signal for the same model, allowing these scenarios to be studied comprehensively.

A variety of experimental approaches are also motivated by rich dark sectors. A dark sector that possesses a large number of particles and interactions can modify many of the relationships used in defining the target parameter spaces listed above, and this can lead to new signatures that can appear in all types of dark-sector experiments. To ensure broad coverage of such signatures, we advocate the development of new avenues of communication between theorists and experimentalists to ensure that, where possible, existing experiments adopt strategies that broaden, rather than narrow, their sensitivities to new particles and interactions. It is also important to develop new computational tools that can facilitate experimental studies of rich dark sectors and provide a link between experimental signatures and astrophysical and cosmological properties of dark sector models.

III. VISIBLE DARK PHOTONS

Conveners: Jim Alexander, Maxim Perelstein. Organizer Contact: Tim Nelson

A. Theory Summary

The Standard Model (SM) of particle physics describes strong, weak and electromagnetic interactions in terms of a gauge theory based on the $SU(3) \times SU(2) \times U(1)_Y$ symmetry group. While phenomenologically successful, the model does not provide insight into the origin of this symmetry. It is quite possible that a more complete theory of nature will include additional gauge interactions. Additional gauge groups appear in many theoretical extensions of the SM, such as supersymmetric models, string theory, and many others. In addition, the existence of dark matter motivates extending the SM to include a "dark sector", consisting of fields with no SM gauge charges. The dark sector may well include additional gauge symmetries. In fact, as discussed in the Introduction, an abelian gauge boson of the dark sector can provide a natural "portal" coupling the dark sector with the SM. This motivates experimental searches for non-SM gauge bosons associated with such extended symmetry structures. This section will discuss such experimental searches. Our focus will be on accelerator experiments looking for gauge bosons with masses roughly between 1 MeV and 10 GeV. The lower bound of this range is defined primarily by the existing bounds from accelerator experiments, cosmology, and astrophysics. The upper bound is dictated by the kinematic reach of the high-intensity accelerator facilities considered here. Of course, these searches are complemented by the experiments at energy frontier facilities such as the LHC, which are sensitive to extra gauge bosons with higher masses, up to a few TeV, albeit with lower sensitivity.

Collider experiments searching for non-SM gauge bosons must rely on their couplings to SM particles, primarily electrons and quarks, to produce them. In the simplest picture, such couplings arise from the "kinetic mixing" interaction, which mixes the gauge boson of a non-SM "dark" gauge group $U(1)_D$ with the SM photon:[198]

$$\mathcal{L}_{\text{kin.mix.}} = \frac{1}{2}\epsilon F^{\mu\nu} F'_{\mu\nu}. \tag{11}$$

Here F and F' are field strength tensors of the SM $U(1)_{\text{em}}$ and the dark $U(1)_D$, respectively, and ϵ is a dimensionless parameter. This coupling generically arises in theories that include new fields charged under both $U(1)_D$ and $U(1)_{\text{em}}$. If the kinetic mixing appears at the one-loop level, ϵ can be estimated to be in the range $\sim 10^{-2} \ldots 10^{-4}$. In some cases, the one-loop contribution to the kinetic mixing may vanish; for example, this occurs if the heavy states that induce it appear in multiplets of an $SU(5)$ or a larger GUT group. In this case, the leading contribution is two-loop, and $\epsilon \sim 10^{-3} \ldots 10^{-5}$, with values as low as 10^{-7} possible if both $U(1)$'s are in unified groups. Notice that since kinetic mixing is a relevant operator, these estimates are independent of the mass of the heavy particles that give rise to it. The physical consequences of the kinetic mixing are best understood in the basis where the kinetic terms are canonical. In this basis, the theory contains two gauge bosons, the ordinary photon A and the dark photon A'. The interactions between the dark photon and SM particles are described by

$$\mathcal{L}_{\text{int}} = \epsilon\, e A'_\mu J^\mu_{\text{EM}}\,, \tag{12}$$

where J^μ_{EM} is the usual electromagnetic current, so that the A' couplings to SM particles are proportional to their electric charges. The interaction in (12) is responsible for the

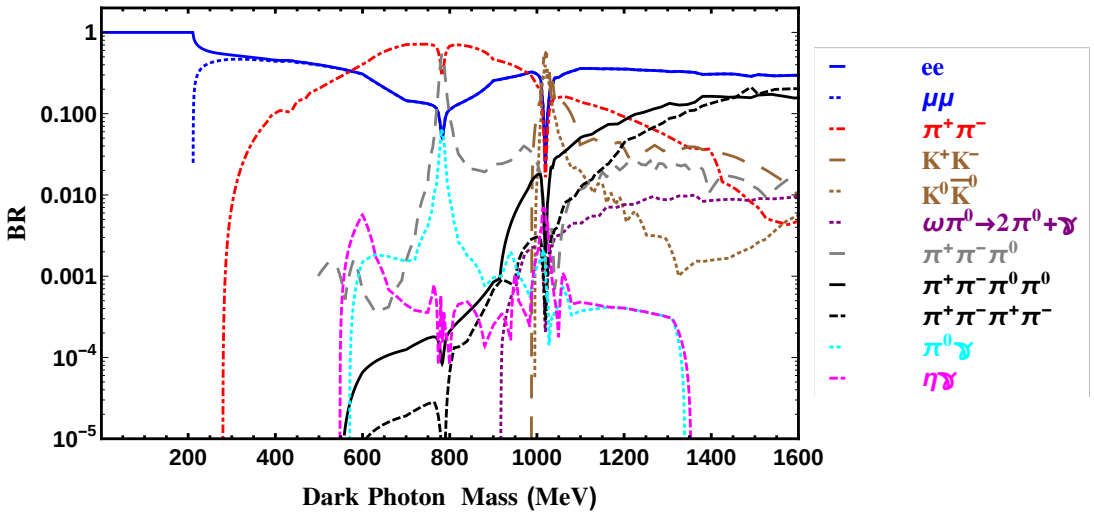

FIG. 1: Visible dark photon decay branching ratios. (Figure from Ref. [24].)

production of dark photon in SM particle collisions, and for its decays into SM states. The simple structure of the interaction leads to a highly predictive theory: for example, the predicted branching ratios of A' decays are shown in Fig. **??**.

In addition, the dark photon may couple to other non-SM particles in the dark sector: for example, there may be new matter states charged under $U(1)_D$, which may include particles that constitute dark matter. If decays of the dark photon to the dark sector states are kinematically forbidden, such couplings are irrelevant to the phenomenology of the experiments discussed here, and the branching ratios of Fig. **??** hold. This case is referred to as the *"visible dark photon"* model. If, on the other hand, the dark photon can decay into dark sector states, the branching ratios into the SM would be (uniformly) reduced. In the simplest case, the dark sector decays of the A' would not be seen by the standard particle detectors, and are referred to as "invisible".[199] Such invisible decays can nevertheless be detected by using missing-mass or missing-momentum techniques, see below. Depending on the model of the dark sector, A' decays into mixed final states containing both SM and dark sector particles are also possible. The large variety of possible final states puts a premium on search approaches that are insensitive to the specific decay channel, such as the missing-mass technique.

B. Strategies for Dark Photon Searches

Current and planned dark photon searches can be characterized by their strategies for production and detection of the dark photon. The main production channels include:

- **Bremsstrahlung:** e^- Z $\to$ e^- ZA', for electrons incident on a nuclear target of charge Z. In a fixed-target configuration the A' is produced very forward, carrying most of the beam energy (for $E_{\rm beam} \gg m_{A'}$) while the electron emerges at a larger angle. Acceptance for the forward-moving A' can be nearly complete; high-resolution spectrometers with lower acceptance require higher-current beams. Mass reach extends

nominally up to beam energy but falls rapidly with mass. Proton-beam fixed-target experiments also exploit bremsstrahlung production, $\mathrm{p\,Z} \to \mathrm{p\,Z}A'$.

- **Annihilation:** $e^+e^- \to \gamma A'$. This production process is favored for searches that emphasize invisible A' decay modes, in which the unseen A' is reconstructed as a missing-mass; visible modes can also contribute. Annihilation channels are pursued in both fixed-target experiments with e^+ beams, and e^+e^- collider experiments. The accessible A' mass is limited by $\sqrt{s}$.

- **Meson decay:** Dalitz decays, $\pi^0/\eta/\eta' \to \gamma A'$, and rare meson decays such as $K \to \pi A'$, $\phi \to \eta A'$, and $D^* \to D^0 A'$, may produce low-mass dark photons if their coupling to quarks is nonzero. Hadronic environments, either in colliders or fixed-target setups, offer copious meson production and make this a favored production channel. The rare meson decay mechanism plays a role in e^+e^- colliders: $e^+e^- \to \phi$ (KLOE, KLOE-2) and $e^+e^- \to \Upsilon(3S)$ (Babar). The A' mass reach is limited by the parent meson mass.

- **Drell-Yan:** $q\bar{q} \to A' \to (\ell^+\ell^-$ or $h^+h^-)$. This process is useful in hadron colliders and proton fixed-target experiments.

The methods of A' detection may be broadly summarized as follows:

- **Bump hunt in visible final state invariant mass:** $A' \to \ell^+\ell^-$ or $A' \to h^+h^-$ against high background. Firm control of statistical and systematic issues is necessary to achieve reliable results when S/B may be in the $10^{-4} \sim 10^{-6}$ range.

- **Bump hunt in missing-mass:** In $e^+e^- \to \gamma A'$ or meson decay production channels, invisible A' decay may be detected indirectly as a bump in a missing-mass distribution. The visible SM part of the final state is reconstructed; the initial state must be known. The same challenges as noted above apply to missing-mass bump hunts.

- **Vertex detection** in $A' \to \ell^+\ell^-$. The A' decay length scales with $(\varepsilon^2 M_{A'})^{-1}$, implying that searches for displaced vertices in visible decay modes probe the very low-ε regions of parameter space. Experiments with vertex reconstruction also do visible invariant mass bump hunts.

The three detection strategies listed above correlate with regions of the $(\varepsilon^2, m_{A'})$ parameter plane. This is illustrated in Figure 1, which shows a cartoon of the sensitivity regions for the three generic experimental approaches. The rightward direction corresponds to available kinematic reach; reach in the downward direction is determined by integrated luminosity; the diagonal direction corresponds to increasing decay length. The gap between regions A and B, which has come to be called "Mont's Gap" after JLAB Director Hugh Montgomery's complaint that HPS coverage in coupling strength was incomplete, highlights the challenge to fill in the transition region between bump hunts and displaced vertex searches by either increased luminosity (for bump hunts) or improved vertex resolution for short decay lengths, or both.

C. Thumbnail summaries of ongoing and proposed experiments

We summarize briefly the main features of the current and proposed experiments searching for dark photons by any or all of the above techniques.

Electron Beams:

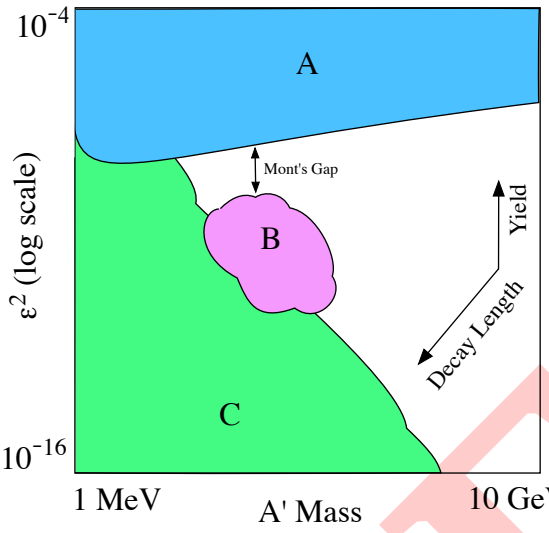

FIG. 2: Cartoon of ε^2 vs. A' mass parameter plane. Region A: bump hunts, visible or invisible modes. Region B: displaced vertex searches, short decay lengths; Region C: displaced vertex searches, long decay lengths.

- **APEX:** Production is by electron-bremsstrahlung, in Jefferson Lab's Hall A, with 120μA. The experiment uses a high-resolution pair spectrometer with low acceptance, $\sigma_M/M \sim 0.5\%$, covering a A' mass range $65 < m_{A'} < 600$ MeV. Detection strategy is the $m_{A'}$ bump hunt. First publication was in 2010, with 2nd run scheduled for 2018. References: [25, 26].

- **A1:** Production by electron bremsstrahlung, in the Microtron beam at Mainz (180-855 MeV; 100μA). Using a high resolution spectrometer, the experiment conducts a bump hunt in visible decays $A' \to e^+e^-$. The parameter coverage is 40MeV $< m_{A'} <$ 300MeV, with ε^2 reaching to 8×10^{-7}. First publication was in 1011. Future plans include a possible upgrade to include displaced-vertex reconstruction. References: [27, 28]

- **HPS:** Production by electron-bremsstrahlung, $20-200$ MeV $m_{A'}$ reach, $1-2$ MeV $m_{A'}$ resolution. The experiment is performed in the CEBAF e^- beam with $50-500$nA current in the range $1-6$ GeV. The experiment has high acceptance and vertex detection by silicon trackers, with vertex resolution in the range $1-5$ mm, depending on $m_{A'}$. Data taking has started, with first publications expected in 2016, 2017; upgrades are envisioned for 2018, together with higher beam energies; 10% of the allocated run time has been used. Two search strategies are employed: $m_{A'}$ bump hunt, and displaced vertex detection, leading to two exclusion islands in the darkplane. Anticipated upgrades aim to close Mont's Gap with improved vertexing and increased luminosity. References: [29].

- **DarkLight:** Production by electron-bremsstrahlung, in the JLab Low-Energy Recirculator Facility with an electron beam of 10mA at 100 MeV. The experiment uses a windowless gas target in the recirculating beam, searching for the visible $A' \to e^+e^-$

final state. A silicon layer detects the recoil proton, implying possible sensitivity to invisible decays (ie fully-known initial state). Initial engineering run (2012) demonstrated the use of the internal gas target; the next stage (2016) will include operation of the solenoid, with future runs adding detector elements. References: [30, 31].

- **MAGIX:** Production by electron-bremsstrahlung in the future ERL beam MESA, designed for 1mA current at 155MeV, with a projected luminosity of $\mathcal{L} \sim 1 \times 10^{35}$. The experiment will use a windowless gas-jet or cluster-jet target and deploy a high resolution spectrometer to reconstruct e^+e^- final states. It is expected to probe a mass range 10MeV $< m_{A'} <$ 60MeV with ε^2 reaching to 3×10^{-9} at lower masses. As with DarkLight, the possibility to observe the recoil proton from the initial bremsstrahlung event opens the door to a missing-mass approach and sensitivity to invisible decay modes. Reference: [**?**].

- **"SuperHPS":** Production by electron-bremsstrahlung, using the proposed DASEL electron beam at SLAC. Reference: [**?**].

- **"TBD":** Production by electron-bremsstrahlung, using the Cornell-BNL FFAG-ERL Test Accelerator (CBETA) high-intensity electron ring under construction at Cornell. Expected machine parameters are I=100mA at 76MeV, I=80mA at 146MeV, I=40mA at 286MeV. Reference: [32].

Positron Beams:

- **VEPP3:** e^+e^- annihilation production in 500 MeV circulating e^+ beam with internal hydrogen gas target providing $\mathcal{L} = 10^{33}\,\mathrm{cm}^{-2}\mathrm{s}^{-1}$. The $m_{A'}$ range is $5 - 22$ MeV, with mass resolution $\sim$ 1MeV. missing-mass mode reconstruction allows inclusive detection of invisible A' decays, with visible decays also possible; detection is by missing-mass bump hunt. First run is anticipated for 2019-2020. References: [33, 34]

- **PADME:** e^+e^- annihilation production by 550 MeV e^+ beam incident on thin, active diamond target. The experiment is sensitive to invisible decays, detected by bump hunt in the A' missing-mass distribution; visible modes are also detected and explicitly reconstructed. A' mass reach is up to 24 MeV. Rich final states such as $e^+e^- \to h'A' \to A'A'A'$ will also be searched for. First run is anticipated for end 2018, with a possible future upgrade to 1 GeV beam energy. References: [35]

- **MMAPS:** e^+e^- annihilation production with 6.0 GeV e^+ beam of 2nA incident on thick beryllium target. Expected luminosity is $\mathcal{L} = 10^{34}\,\mathrm{cm}^{-2}\mathrm{s}^{-1}$. As with VEPP3 and PADME, detection is via the missing-mass mode, providing sensitivity to both invisible and visible final states. A' mass reach is $20 - 78$ MeV, with $m_{A'}$ resolution $10 - 1$ MeV over the same range. No first-run date is set yet.

e^+e^- Colliders:

- **BELLE-II:** e^+e^- annihilation at $\sqrt{s} \sim 10$ GeV with sensitivity to visible ($\gamma\ell^+\ell^-$) and invisible (mono-photon) modes. Belle-II will also search for rich final states $e^+e^- \to h'A' \to A'A'A'$. Trigger strategies are under active development for monophoton modes, taking advantage of Belle-II's no-projective-cracks design. The range of sensitivity in A' mass is 20MeV $-$ 10GeV. References: [36].

- **KLOE2:** Production modes include meson decay ($\phi \to \eta A'$), annihilation ($e^+e^- \to A'\gamma$), and dark-higgstrahlung ($e^+e^- \to A'h'$). The DAϕNE-2 upgrade triples previous luminosity, and KLOE2 upgrades include tracking GEM vertex detector and forward calorimetry. Searches include both visible ($A' \to e^+e^-$, $\mu^+\mu^-$, $\pi\pi$) and invisible A' decay modes. Parameter reach in KLOE is $\varepsilon^2 < 1 \times 10^{-5} \sim 1 \times 10^{-7}$, while KLOE2/DA$\phi$NE 2 will improve limits by x2. References: [37–42].

Proton Beams:

- **SeaQuest:** 120 GeV protons on target from FNAL Main Injector. Dark photon production is by DY, meson decay, and proton-bremsstrahlung. The A' search will look for muon pairs emerging from a beam dump; the primary signal is a bump in the dimuon mass distribution, with vertex requirements helping to suppress backgrounds. A parasitic run in 2017 with slightly augmented triggering and electromagnetic calorimetry will establish baseline performance. Further running with more extensive upgrades for particle ID could follow. The expected range of sensitivity is 200MeV $< m_{A'} <$ 10GeV for the bump-hunt mode, and up to 2GeVfor the displaced vertex mode. Reference: [**?**]

- **SHIP:** An ambitious, broad-spectrum search for hidden particles, using the 400GeVproton beam from the CERN SPS. For dark photons, production can be accomplished by proton Bremsstrahlung, DY, QCD Compton scattering, and meson decay. SHIP is sensitive to visible final states with long decay lengths ($\sim$10's m) producing a displaced-vertex signature. Dark photon parameter sensitivity is in the range $10^{-18} < \varepsilon^2 < 10^{-8}$ and $m_{A'} <$ 10GeV, covering an extensive zone in the displaced vertex lobe. The projected running period is 2026-2031, with an integrated accumulation of 2×10^{20} protons on target. Reference: [43].

Proton-proton collisions:

- **LHCb** Notable production mechanisms include exclusive rare heavy quark decay modes such as $D^* \to D^0 A'(\to e^+e^-)$ and $B \to K^* A'(\to \mu^+\mu^-)$ for low mass coverage, $m_{A'} <$ 140MeV. Inclusive visible decays $A' \to \mu^+\mu^-$, with and without displaced-vertex reconstruction provide sensitivity to tens of GeV, punctuated by exclusion zones to remove known resonances. Triggerless operation foreseen in the upgrade for LHC Run 3 (2021-2023) and beyond is expected to increase sensitivity reach substantially. References: [44–46].

D. Projections for future experiments

Figures 3 and 4 illustrate the dark photon parameter plane, ε^2 versus $m_{A'}$, with existing exclusion zones indicated in gray, and anticipated exclusion reaches of planned experiments indicated by colored curves. Table III D summarizes actual and/or projected performance and characteristics of dark photon experiments.

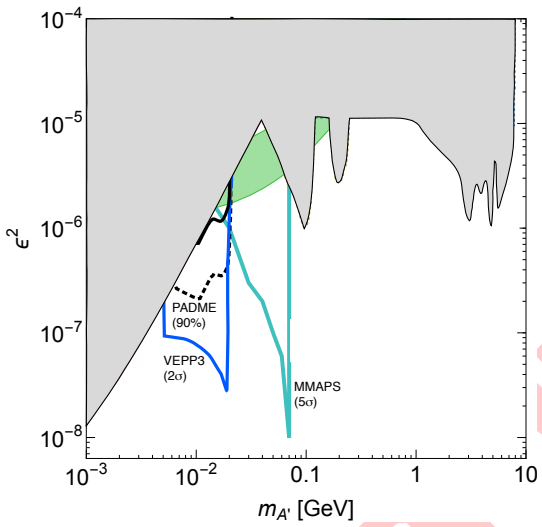

FIG. 3: A' sensitivity for missing-mass experiments, allowing invisible decay modes. Existing exclusions, shown in gray, have been smoothed.

E. Summary of ongoing and proposed experiments

The experimental community for dedicated dark sector searches has grown substantially in the last eight years and as the list above illustrates, the experiments, whether ongoing or proposed, have expanded to cover a wide range of production modes and detection strategies. Experiments like APEX, A1, HPS, and DarkLight, that take advantage of explicit final state reconstruction, push deep into the ε^2 parameter range, with sensitivity in $m_{A'}$ up to a few hundred MeV. In the coming years, experiments like VEPP3, PADME, and MAPPS will address a more limited parameter range, but as missing mass experiments, eliminate aspects of model dependence by being fully agnostic as to the final state. Collider experiments allow probes to much higher masses than can be reached in fixed-target experiments. Some, like Belle-II and LHCb, will have trigger schemes specifically optimized for dark sector searches. Taken together, the set of existing and planned experiments form a suite of balanced and complimentary approaches, well suited to the search for new phenomena whose physical characteristics and potential manifestations cannot be predicted in detail ahead of time.

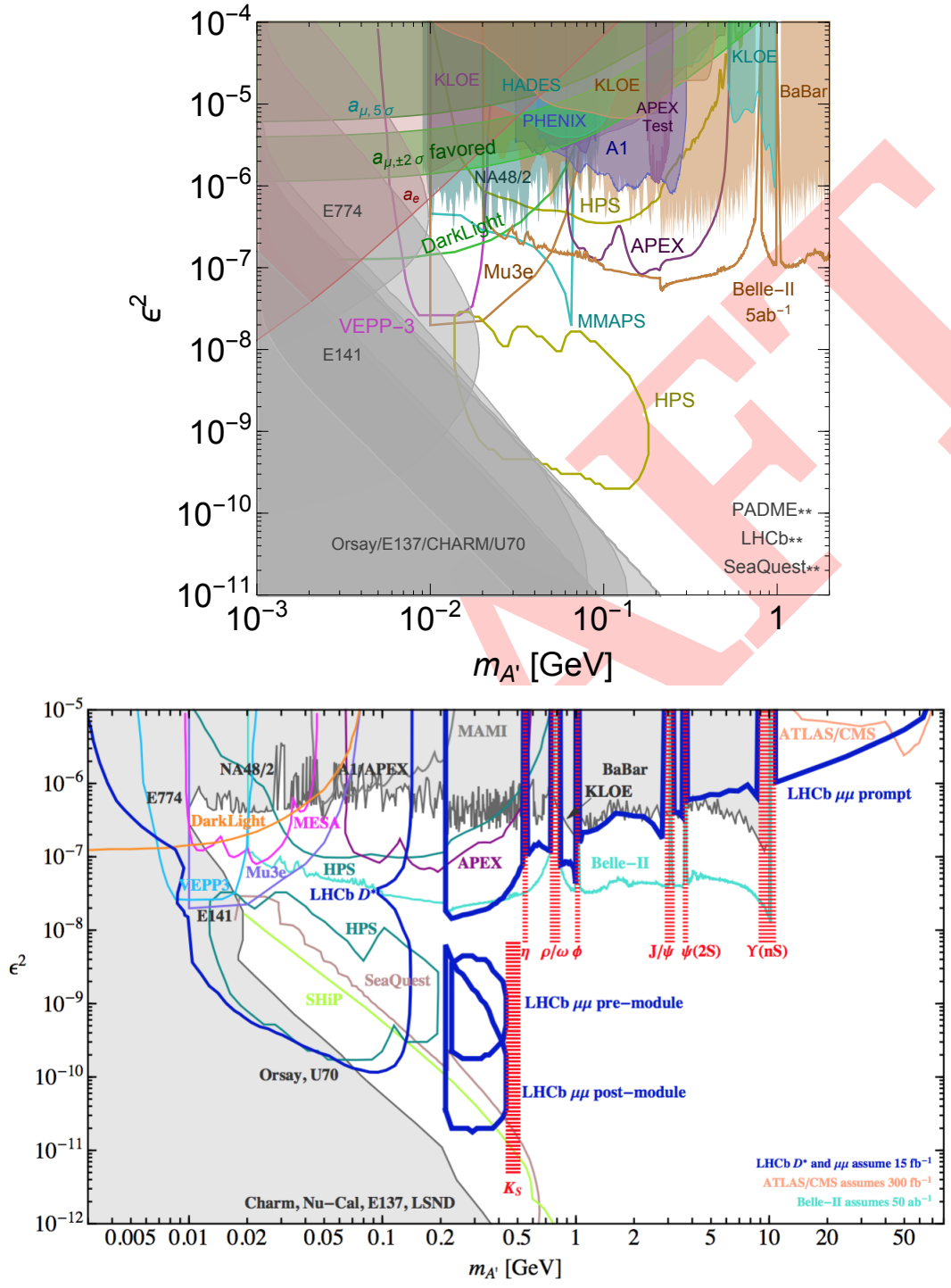

FIG. 4: (Placeholder) A' sensitivity for exclusive experiments seeking visible decay modes $A' \to \ell^+\ell^-$. Top plot: Experiments capable of delivering results over the next 5 years to 2021. Bottom plot: Longer term prospects beyond 2021 for experimental sensitivity.

TABLE I: Summary of dark photon experiments.

Experiment	*Lab*	*Production*	*Detection*	*Vertex*	*Mass(MeV)*	*Mass Res. (MeV)*	*Beam*	*Ebeam (GeV)*	*Ibeam or Lumi*	*Machine*	*1st Run*	*Next Run*
APEX	JLab	e-brem	$\ell^+\ell^-$	no	$65-600$	0.5%	e^-	1.1–4.5	150μA	CEBAF(A)	2010	2018
A1	Mainz	e-brem	e^+e^-	no	$40-300$	?	e^-	0.2–0.9	140μA	MAMI	2011	–
HPS	JLab	e-brem	e^+e^-	yes	$20-200$	1–2	e^-	1–6	50–500nA	CEBAF(B)	2015	2018
DarkLight	JLab	e-brem	e^+e^-	no	< 80	?	e^-	0.1	10mA	LERF	2016	2018
MAGIX	Mainz	e-brem	e^+e^-	no	$10-60$	?	e^-	0.155	1mA	MESA	2020	–
(TBD)	SLAC	e-brem	vis	yes	< 500	?	e^-	$4-8$	1μA	DASEL	?	?
(TBD)	Cornell	e-brem	e^+e^-	?	< 100	?	e^-	0.1-0.3	100mA	CBETA	?	?
VEPP3	Budker	annih	invis	no	$5-22$	1	e^+	0.500	$10^{33}\,\mathrm{cm}^{-2}\mathrm{s}^{-1}$	VEPP3	2019	?
PADME	Frascati	annih	invis	no	$1-24$	$2-5$	e^+	0.550	$\leq 10^{14} e^+$OT/y	Linac	2018	?
MMAPS	Cornell	annih	invis	no	$20-78$	$1-6$	e^+	6.0	$10^{34}\,\mathrm{cm}^{-2}\mathrm{s}^{-1}$	Synchr	?	?
KLOE 2	Frascati	several	vis/invis	no	< 1.1GeV	1.5	e^+e^-	0.51	$2\times10^{32}\,\mathrm{cm}^{-2}\mathrm{s}^{-1}$	DAϕNE	2014	-
Belle II	KEK	several	vis/invis	no	$\lesssim 10$GeV	$1-5$	e^+e^-	4×7	$1\sim10\,\mathrm{ab}^{-1}$/y	Super-KEKB	2018	-
SeaQuest	FNAL	several	$\mu^+\mu^-$	yes	$\lesssim 10$GeV	$3-6\%$	p	120	10^{18} POT/y	MI	2017	2020
SHIP	CERN	several	vis	yes	$\lesssim 10$GeV	$1-2$	p	400	2×10^{20} POT/5y	SPS	2026	-
LHCb	CERN	several	$\ell^+\ell^-$	yes	$\lesssim 40$GeV	~ 4	pp	6500	$\sim 10\,\mathrm{fb}^{-1}$/y	LHC	2010	2015

IV. DARK MATTER AT ACCELERATORS

Conveners: Marco Battaglieri, Eder Izaguirre, Gordan Krnjaic, Richard G Van De Water. Organizer Contact: Philip Schuster

A. Theory Summary

In this section we motivate the broad class of light dark matter (LDM) models coupled to the Standard Model (SM) through a new light mediator. We describe the simple models that can accommodate all existing data. Moreover, we give an overview of the capabilities of present, and near future proposals to make experimental progress in the field.

In many models, dark matter particles do not have direct couplings to the Standard Model. Instead, they interact with the SM through a "mediator", a particle that couples to both the SM and the DM. In this section, we will focus on the models where both the DM particle and the mediator are relatively light, in the sub-GeV mass range. The gauge and Lorentz symmetries of the SM greatly restrict the ways in which the mediator can couple to the SM. One expects the dominant interactions to be the so-called renormalizable portals: those interactions consisting of SM gauge singlet operators with mass dimension < 4:

$$\hat{\mathcal{O}}_{\rm portal} \;=\; H^\dagger H \quad , \quad LH \quad , \quad B_{\mu\nu} \quad , \tag{13}$$

and a new SM-neutral degree of freedom, which can be a scalar ϕ, a fermion N, or a vector A'. Here H is the SM Higgs doublet with charge assignment $(1, 2, +\frac{1}{2})$ under the SM gauge group $SU(3)_c \times SU(2)_L \times U(1)_Y$, L is a lepton doublet of any generation transforming as $(1, 2, -\frac{1}{2})$, and $B_{\mu\nu} \equiv \partial_\mu B_\nu - \partial_\nu B_\mu$ is the hypercharge field strength tensor. Although there could also be higher dimension effective operators to connect to the mediators, direct searches for the states that resolve such operators require suppression scales in excess of the electroweak scale, which generically would lead to over-abundance of dark matter if these were the predominant interactions that set the DM relic abundance.

If the mediator is a scalar particle ϕ, the only allowed renormalizable interactions are through the Higgs portal via $\phi H^\dagger H$ and $\phi^2 H^\dagger H$ which induce mass mixing between ϕ and the SM Higgs boson after electroweak symmetry breaking. The simplest example in this scenario, however, is already sharply constrained by existing experiments [3]. If the mediator is a fermion N, its interaction with the SM proceeds through the neutrino portal $\sim y_\nu LHN$ and it plays the role of a right handed neutrino with a Yukawa coupling y_ν. If DM is *not* thermal in origin, N can itself be a viable, cosmologically metastable DM candidate in a narrow mass range [4]. Since N is stipulated to be sub-GeV, obtaining the observed neutrino masses (without additional field content) requires Yukawa couplings of order $y_\nu \lesssim 10^{-7}$, which are too small to allow thermalization to take place at early times [47]. We note the possibility that N is the mediator, but not the DM; in this case additional particle content in the dark sector would be needed to accommodate DM.

We, thus, focus on the third scenario, as it's the most viable for models of light DM. If the mediator is a vector force carrier from an additional $U(1)_D$ gauge group under which LDM is charged, the "kinetic mixing" interaction $\epsilon_Y B^{\mu\nu} F'_{\mu\nu}$ is gauge invariant under both $U(1)_D$ and $U(1)_Y$. Here ϵ_Y is, *a priori* a free parameter, though it often arises in UV complete models after heavy states charged under both groups are integrated out at a high scale, so it is generically expected to be small, $\epsilon_Y \sim 10^{-3}$ or smaller [7]. Additionally, important variations, such as the scenarios where the mediator couples preferentially to baryonic, or

leptonic, or $(B-L)$ currents, respectively, have a phenomenology that is similar to the kinetic mixing scenario. And finally, the nature of the DM particle content is important. In particular, it could have diagonal or off-diagonal (majorana-like) couplings to the mediator, which can affect the phenomenology (see Ref. [8] for an example), or it could live in a rich sector (*e.g.,* see Ref. [9]). Additionally, the spin of DM is important as cosmological bounds are more severe for spin 1/2 DM since its direct annihilation into the SM is s-wave suppressed. In contrast, spin 0 DM annihilation into the SM is $p-wave$ suppressed and thus does not suffer from such severe bounds. In what follows we consider the two scenarios of scalar/fermion DM communicating with the SM through a vector mediator.

B. Defining thermal targets

For all mediators and LDM candidates χ, there is a basic distinction between "secluded" annihilation to pairs of mediators (via $\chi\chi \to$ MED MED for $m_\chi > m_{\rm MED}$) followed by mediator decays to SM particles [17], and "direct" annihilation to SM final states (via virtual mediator exchange in the s-channel, $\chi\chi \to {\rm MED}^* \to$ SM SM for $m_\chi < m_{\rm MED}$) without an intermediate step. For concreteness, the discussion below leading up to the definition of a thermal target is made for fermionic DM. A similar discussion is applicable for scalar DM, up to the difference between p-wave and s-wave annihilation.

For the secluded process, the annihilation rate scales as

$$\text{("secluded" annihilation)} \qquad \langle\sigma v\rangle \sim \frac{g_D^4}{m_\chi^4} \ , \tag{14}$$

where g_D is the coupling between the mediator and the LDM, and there is no dependence on the SM-mediator coupling $g_{\rm SM}$. Since arbitrarily small values of $g_{\rm SM}$, the SM-mediator coupling, can be compatible with thermal LDM in this regime, the secluded scenario does not lend itself to decisive laboratory tests.

The situation is markedly different for the direct annihilation regime in which $m_\chi < m_{\rm MED.}$. Here the annihilation rate scales as

$$\text{("direct" annihilation)} \quad \langle\sigma v\rangle \sim \frac{g_D^2\, g_{\rm SM}^2\, m_\chi^2}{m_{\rm MED}^4} \ , \tag{15}$$

and offers a clear, predictive target for discovery or falsifiability since the dark coupling g_D and mass ratio $m_\chi/m_{\rm MED}$ are at most $\mathcal{O}(1)$ in this $m_{\rm MED} > m_\chi$ regime. Thus, there is a minimum SM-mediator coupling compatible with a thermal history; larger values of g_D require nonperturbative dynamics in the mediator-SM coupling or intricate model building.

In the direct annihilation regime, the minimum annihilation rate requirement translates into a minimum value of the dimensionless combination

$$\boxed{\frac{g_D^2\, g_{\rm SM}^2}{4\pi}\left(\frac{m_\chi}{m_{\rm MED}}\right)^4 \gtrsim \langle\sigma v\rangle_{\rm relic}\, m_\chi^2 \ ,} \tag{16}$$

which, up to order one factors, is valid for every DM/mediator variation provided that $m_{\rm DM} < m_{\rm MED.}$.

DM searches at accelerators can be divided into two broad categories: fixed-target and collider experiments. We summarize the different strategies in Table. II.

Experiment Class	Production Modes	Detection
B-factory	$e^+e^- \to \gamma A'$	missing mass
Electron fixed-target	$e^- Z \to e^- Z A'$	DM scatter or missing energy/mass
Hadron collider	$pp \to (\text{jet}/\gamma)\text{A}'$	missing energy
Positron fixed-target	$e^+e^- \to \gamma A'$	missing mass
Proton fixed-target	$\pi^0/\eta/\eta' \to \gamma A'$, $q\bar{q} \to A'$, $pZ \to pZA'$	DM scatter downstream

TABLE II: Catalogue of complementary experimental strategies to search for light DM.

Existing constraints have primarily been deduced by recasting a number of prior experimental searches. Before moving to future opportunities, we provide a brief summary of these limits. For lower mass DM, the strongest constraints follow from limits on anomalous scattering at proton and electron fixed target experiments such as LSND [48–50] and E137 [51, 52]. For specific mass ranges, limits on invisible pion [53], kaon [14, 54] and J/Ψ [55] decays are significant, while monophoton searches at BaBar [56, 57] are stringent at higher masses, while monojet searches [58, 59] are generally less constraining, but relevant for leptophobic mediators. Finally, vector mediator exchange induces corrections to $g-2$ of the electron and muon, which impose constraints at low mass [14, 60–62] and, in the case of the muon $g-2$ anomaly, have identified a region of interest in parameter space. A number of these existing limits are shown in the figures below.

In what follows, we elaborate on current and future opportunities.

C. Proton beam-dump experiments

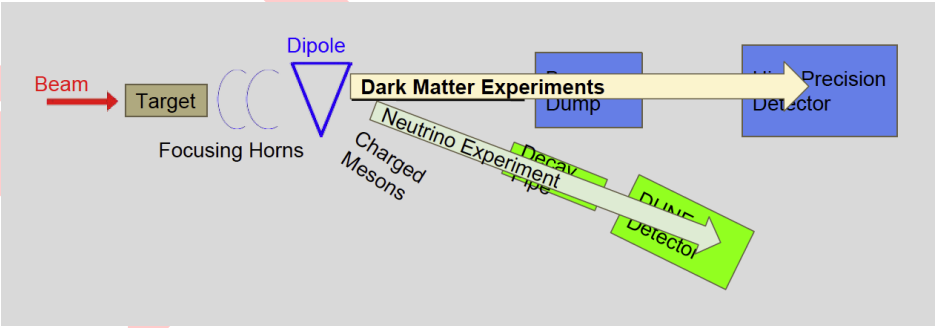

FIG. 5: Schematic of the dual purpose LBNF beam-line that can simultaneously produce both a charged and neutral beam. The charge beam decays into neutrinos while the neutral beam can couple to LDM.

- **MiniBooNE at FNAL**: 8 GeV BNB protons. Can run in target mode (Be), and off-target mode (Fe). Mineral oil Cherenkov detector, 450 ton fiducial mass, situated 540 m downstream. Main production mode via $\pi^0/\eta\eta' \to \gamma(A' \to \chi\bar{\chi})$ and $q\bar{q} \to A' \to \chi\bar{\chi}$. Detection via $\chi e \to \chi e$, or $\chi N \to \chi N$ elastic scattering, or via inelastic such as $\chi N \to \chi(\Delta \to N\pi^0)$. Completed running in off-target mode with 1.86×10^{20} POT, analysis ongoing. See Ref. [9, 48, 49, 63–68] for more details.

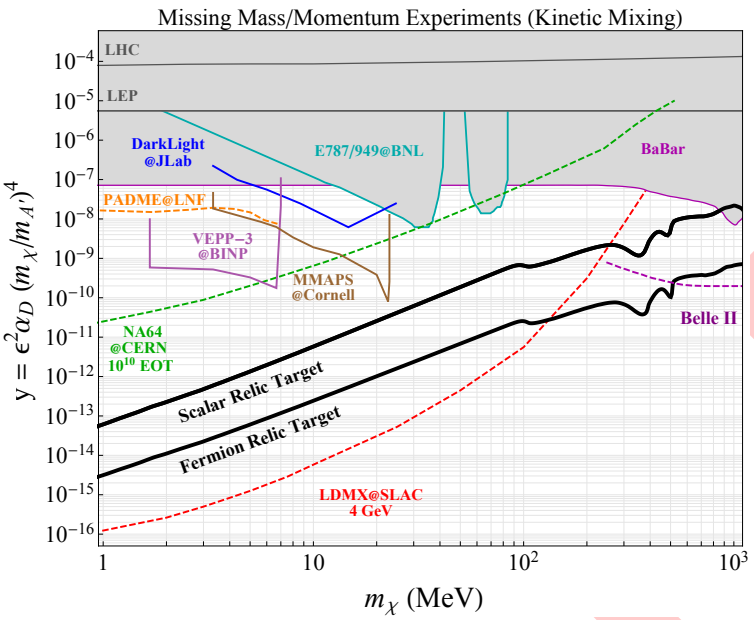

FIG. 6: Yield projections for various proposed DM search strategies involving missing mass/momentum plotted alongside constraints based on the same experimental technique and the thermal target for scalar and fermion DM candidates. Here all bounds and projections conservatively assume $m_\chi = 3\,m_{A'}$, but the thermal targets are invariant as this ratio changes. For larger ratios, the experimental curves shift downward to cover more parameter space; for small ratios $m_\chi > 3m_{A'} <$, there is no thermal target as the DM annihilation proceeds trough $\chi\chi \to A'A'$ annihilation which is independent of the SM coupling ϵ, This plot serves to compare proposed missing momentum based searches against similar constraints; bounds not based on missing momentum techniques (e.g. direct detection or beam dump searches) are omitted. Here, the shaded regions represent excluded parameter space, dashed projections are based on signal-yield estimates and solid curves represent actual sensitivity estimates based on background studies.

- **T2K**: 30 GeV protons. The near and far detectors are two degrees off-axis, and the timing structure of the bunches in each spill can be used to cleanly separate beam-related backgrounds at the far-detector, Super-Kamiokande, a 50 kiloton water Cerenkov detector 295km from the target. The production modes are as for MiniBooNE, but the high degree of background reduction can compensate for the reduced angular acceptance in utlizing the far detector. Initial analysis will focus on deexcitation gammas from the neutral current quasielastic (NCQE) interaction on oxygen (see [69] for related studies of neutrino scattering), again testing the underlying $\chi N \to \chi N$ process. The final dataset is expected to be 7.8×10^{21}POT by 2021.

- **SBN at FNAL**: 8 GeV BNB protons. Three Liquid Argon TPC detectors (LArTPC), 112 ton, 89 ton, and 476 ton fiducial mass situated 110 m, 470 m, and 600 m respectively downstream. Production and detection channels as in MiniBooNE. Curernt plan to collect 6×10^{20} POT, beginning in 2018, in on-target mode. Can be configured to collect 2×10^{20} POT in beam-dump mode after on-target run, with expected sensitivity an order of magnitude better than MiniBooNE. Upgrades to BNB in 2016 will enable simultaneous on/off-target running. Significantly improved sensitivity can be achieved with reduction in neutrino background rates by replacing neutrino horn with an iron target.

- **Near Detector at FNAL's LBNF/DUNE**: 120 GeV Protons. 1 MW beam power. Fig. 5 shows the kind of dual purpose facility that can be built for the LBNF neutrino source. A dipole magnet is used to sweep the charge particles, that decay into neutrinos, into a different direction while the neutral beam particles that can couple to LDM continue in the forward direction. This effectively decouples the two beams and produces the most physics reach for both neutrino oscillations and LDM searches. To leverage the investment in the LBNF/DUNE experiment to run simultaneously in beam dump and neutrino mode could be cost effective but will require more funding and design work in the next few years. However, this would provide the ultimate proton beam-dump search. Timeline: $>$ 2020. See Ref. [70] for more details.

- **SHiP**: 400 GeV protons at CERN's SPS. Expected to be able to deliver 10^{20} POT. A neutrino detector consisting of OPERA-like bricks of laminated lead and emulsions, placed in a magnetic field downstream of the muon shield, will allow to measure and identify charged particles produced in charged current neutrino interactions. It is followed by a tracking system and muon magnetic spectrometer. Timeline: $>$ 202X. See Ref. [71].

D. Electron beam-dump experiments

- **BDX at JLab**: 11 GeV CW (ns-spaced bunches) electron beam. Capable of delivering 10^{22} EOT in one year's running to Al dump. BDX detector proposed to be situated 20 m downstream, for which new infrastructure is requested. CsI scintillator, 1 m^3. Main production mode via $e^- Z \to e^- Z(A' \to \chi\bar{\chi})$. Most promising detection via $\chi e \to \chi e$ or $\chi N \to \chi N$. For Majorana-DM models: production via $e^- Z \to e^- Z(A' \to \chi_1\chi_2)$ and detection via $\chi_1(e/Z/N) \to \chi_2(e/Z/N)$ followed by $\chi_2 \to \chi_1 e^+ e^-$ inside detector. Another strategy is to use a different detection technique in the same experiment (e.g. calorimetry and gas-based detectors BDX-DRIFT) to have an independent confirmation of any possible finding. Proposal submitted to JLab's 44th PAC. See Ref. [72, 73]. for more details.

- **BDX-like at SLAC**: 4 GeV LCLS-II beam. Possible to upgrade to 8 GeV in future. Unlike JLab, features 1 MHz repetition bunches. Capable of delivering 3×10^{21} EOT in one year's running to dump. New infrastructure to host the detector is not needed. However, the detector would have to contend with two beam pipes for LCLS-II X-ray beam users carrying a few KHz of high energy pulses past the detector, and the backgrounds must be evaluated. Timeline: $\gtrsim$ 2020.

E. Electron missing energy and momentum experiments

- **VEPP-3 at BINP**: 500 MeV, 500 mA positron beam incident on internal Hydrogen target at the Budker Institute of Nuclear Physics (BINP) in Novosibirsk, Russia [34]. Signal is the missing mass reconstructed from $e^+e^- \to \gamma(A' \to \chi\chi)$ annihilation. Timeline: $\sim$ 2020.

- **MMAPS at Cornell**: 1.8-5.3 GeV, 2.3 nA positron beam incident on a Be target at the Wilson Lab at Cornell University in Ithaca, NY, USA [74]. Signal is the missing

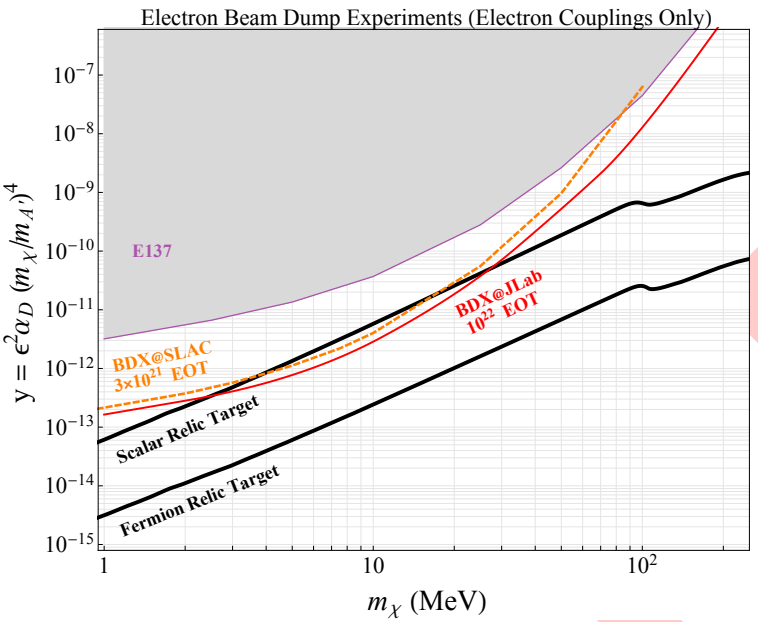

FIG. 7: Same as Fig 6 but for electron beam dump experiments.

mass reconstructed from $e^+e^- \to \gamma(A' \to \chi\chi)$ annihilation. Timeline: TBD

- **Padme at LNF**: 550 MeV positron beam incident on a diamond target at the INFN Laboratory in Frascati, Italy [35]. Signal is the missing mass reconstructed from $e^+e^- \to \gamma(A' \to \chi\chi)$ annihilation. Timeline: $\sim 10^{13} e^+$ on target by the end of 2018.

- **DarkLight at JLab**: 100 MeV Low Energy Recirculating Facility (LERF), formerly the Free Electron Laser, at Jefferson Lab [31]. Missing mass experiment sensitive to $ep \to ep(A' \to \chi\chi)$ by reconstructing full final state kinematics. Beam current of order 5 mA impinges on a windowless gas target of molecular hydrogen. The complete final state including scattered electron, recoil proton, and e^+e^- pair will be detected. Timeline: a phase-I experiment has been funded and is currently taking data. The complete phase-II experiment is under final design and could run within two years after phase-I is completed.

- **NA64 at CERN**: 100 GeV secondary electrons at CERN's SPS. Range of currents: $(1-5) \times 10^5 e^-/s$. Pulse structure: 2-4 spills of 4.8 s per minute. Production mode via $eZ \to eZ(A' \to \chi\bar{\chi})$. The detector consists of: a tracker (MM 1-4) combined with a bending magnet which acts as a spectrometer in order to identify the momentum of the incoming particles. The synchrotron radiation produced by the incoming particles is detected by a BGO detector placed 12 m downstream the magnet which is used to suppress hadron contamination. The particles are dumped in the ECAL where bremsstrahlung photons can be produced. The ECAL is followed by a VETO and a highly hermetic HCAL. The signal is defined as energy deposition in the ECAL below a given energy threshold and no energy deposition in the VETO or the HCAL. Timeline: approved for 2 weeks test beam, and 4 weeks physics run in 2016. Expected to collect 10^{10} EOT.

- **LDMX at SLAC**: 4 GeV LCLS-II beam. Possible to upgrade to 8 GeV in future.

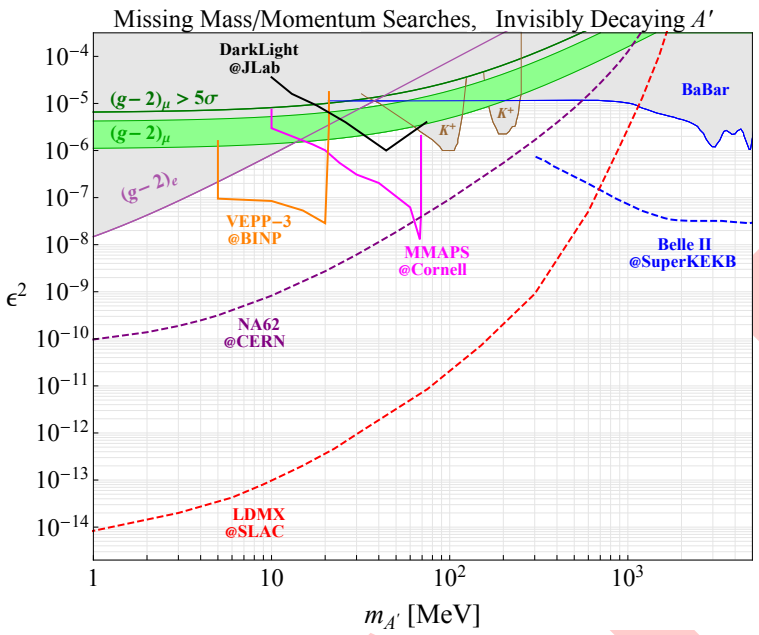

FIG. 8: Parameter space for an invisibly decaying dark photon with mass $m_{A'}$ and kinetic mixing parameter ϵ with no assumptions about its decay products so long as they are invisible on relevant experimental length scales. The shaded regions are model independent constraints from $(g-2)_\mu$ [14], $(g-2)_e$ [75], BABAR [76], E787/E949 [54, 77], and the green band represents the parameter space for which A' resolves the $(g-2)_\mu$ anomaly [14]. Curves corresponding to unshaded regions represent projections for future dedicated searches for invisibly decaying A' using missing mass/momentum techniques also shown in Fig. 6.

Missing momentum experiments propose to detect a $eZ \to eZ(A' \to \chi\bar{\chi})$ by measuring the momentum and energy of the soft outgoing electron, as well as relying on excellent hermiticity to infer the missing energy from the DM particles escaping. The experiment calls for a low current, at $10 - 1000$ MHz, tagging the incoming electron impinging on a thin high Z target. The target is followed by tracking layers to measure the momentum of the outgoing electron, as well as by an electromagnetic and (possibly) a hadronic calorimeter downstream to veto SM reactions which can mimic the one-soft-outgoing electron and missing momentum signal. Timeline: > 2020. See Refs. [78, 79] for more details.

F. High energy colliders

- **Belle-II at SuperKEKB**. e^+e^- asymmetric collider at the Υ resonance ≈ 10.3 GeV. Expected to achieve integrated luminosities of 50/ab (~ 100 times greater than BaBar's), it can look for DM through the reaction $e^+e^- \to \gamma(A' \to \chi\bar{\chi})$. Its signature is a monoenergetic photon. Expected to start collecting data in 2018. See Ref. [80] for more details.

- **LHC at CERN**. Analogously to a B-factory, at the LHC, one can produce DM by looking for $pp \to j(A' \to \chi\bar{\chi})$. In this case, however, one does not look for a bump, but instead for missing energy. For more details, see Ref. [81]. Addtionally, new striking signatures may result in models where the DM is majorana-line. In those models, the

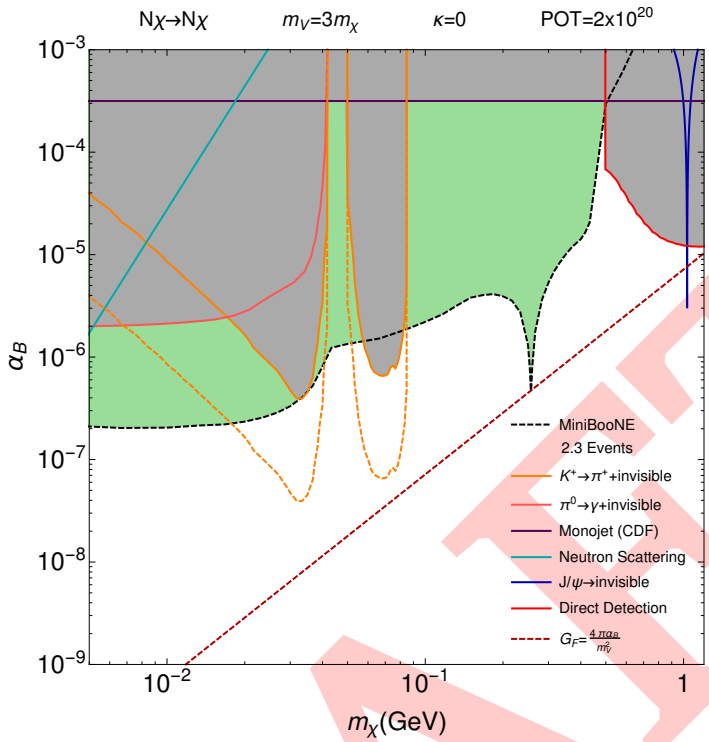

FIG. 9: MiniBooNE yield projection for a leptophobic vector force coupled to dark matter [66]. here the projections are compared against the weak scale benchmark for which $4\phi\alpha_B/mV^2 = G_F$, where α_B is the dark coupling and m_V is the mediator mass.

A' decays via $A' \to \chi_1\chi_2$, with χ_2 possibly giving striking signatures through its decay into $\chi_1(A'^{(*)} \to \ell\ell)$. See, for instance, Refs.[8, 82–85].

G. Projections

In Fig. 6 we show yield projections and sensitivity estimates for various proposed LDM experiments based on missing mass/momentum techniques. plotted against relevant constraints based on comparable $A' \to \not{E}$ searches on the y vs. $m_{A'}$ as described above. In Figs. 7 and 9 we show the analogous figure for electron and proton beam dump experiments assuming only electron and nucleon couplings respectively. In Fig 10 we show the combined projections various techniques plotted in the y vs. $m_{A'}$ parameter space for a kinetically mixed dark photon. Finally, in Fig. 8 we show the projections for the same missing mass/momentum searches presented in Fig. 6, but in the ϵ^2 vs. $m_{A'}$ parameter space without making any assumption about the identity of the A' decay products so long as they are invisible on the length scales probed by each projection and constraint.

H. Outlook

The field of DM residing in a Dark Sector is a thriving one, with accelerated progress in the next 5-10 years possible thanks to a healthy interplay between maturing technologies and theoretical input. One must ask the question: is there *one* experiment that is able to

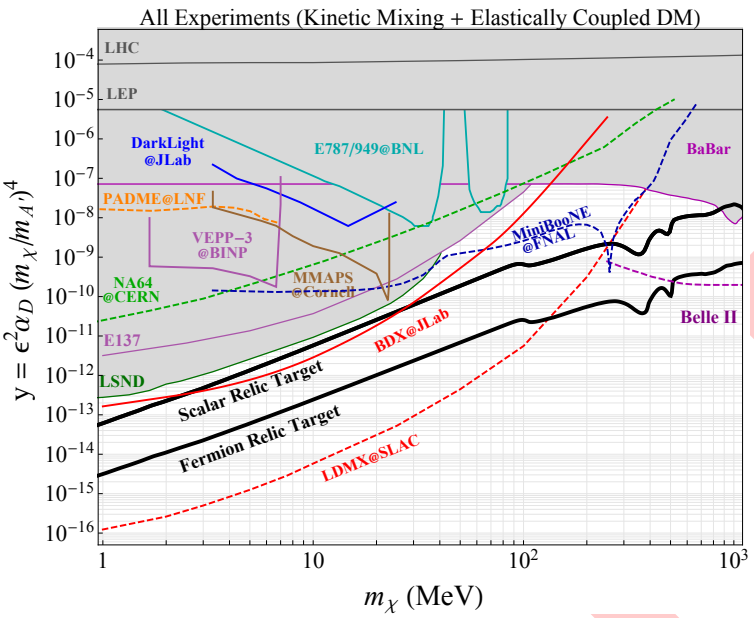

FIG. 10: Combined projections and constraints from Figs. 6, 7, and **??** encapsulating direct production LDM constraints in the context of a kinetically mixed dark photon coupled to an LDM state that scatters elastically (or nearly elastically) at beam dump experiments.

achieve a thorough study of the well-motivated landmarks in the parameter space? The answer, however, is no.

Ignoring the dependence on DM and mediator masses, and focusing on the scenario of the vector portal for concreteness, the experiments that generally will be able to probe the smallest DM-SM interaction couplings are those relying on missing energy, or missing mass — namely, the signal yield in those experiments goes like ϵ^2. Beam-dump experiments, in turn, scale as $\epsilon^4 \alpha_D$, where $\alpha_D \equiv \frac{g_D^2}{4\pi}$. Thus, *within* the vector portal, where the A' couples to all charged SM-fermions democratically, experiments like NA64 and LDMX have the potential to probe the most parameter space for DM and mediator masses below a GeV. However, one must think more generally than about just kinetic mixing. For instance, it's possible to construct models where the mediator couples preferentially to protons [66, 70, 86]; given that possibility, it behooves the community to advocate for performing future proton beam-dump experiments. Similarly, models where the DM is part of a sector where there are heavier but very short-lived excited states — such as the Majorana-like DM scenario with very large mass splittings — are a potential blind spot of experiments like NA64 and LDMX, but a strength of experiments like BDX, or of any of the future proton beam-dump experiments [87]. Finally, for DM and mediator masses above a GeV, Belle-II and the LHC will have stronger sensitivity. Thus, to achieve maximum coverage of the plausible theoretical benchmarks, a combination of these techniques is required.

V. DIRECT DETECTION OF SUB-GEV DARK MATTER

Conveners: Jeremy Mardon, Matt Pyle. Organizer Contact: Rouven Essig

A. Introduction

Among the most important experimental approaches to detecting dark matter (DM) particles in the laboratory are direct detection experiments. Starting with [88], this program has over the last few decades focused on searches for Weakly Interacting Massive Particles (WIMPs), with masses above ~ 10 GeV. The focus has been on searching for *nuclear recoils* induced by WIMPs in the Milky-Way DM halo scattering off nuclei in various target materials. These detectors are placed deep underground and carefully shielded to reduce cosmic-ray and radioactive backgrounds. They employ sensitive equipment, to measure recoils of $\mathcal{O}$(keV) and more, and state-of-the-art target-material fabrication and purification to reduce contaminants that could mimic a DM signal. This program is well-established, important, and has a clear path forward [89]. Nevertheless, as emphasized in this report and elsewhere, the search for DM must be dramatically expanded to capture the range of possible candidates. In particular, dark-sector DM, coupled to new mediators like a dark photon, could have masses well below the GeV scale, making it imperative to develop direct-detection strategies for such low DM masses.

The traditional search for nuclear recoils rapidly looses sensitivity for DM masses, m_χ, below a few GeV. The energy of the recoiling nucleus is given by $E_{\rm NR} \leq 2\mu_{\chi,N}^2 v^2/m_N$, where $\mu_{\chi,N}$ is the reduced mass of the DM and a nucleus of mass m_N. For a xenon nucleus and $m_\chi \sim 100$ MeV, we have $E_{\rm NR} \sim 1$ eV. Currently the lowest nuclear recoil threshold is $\sim 300\,$eV by the CRESST experiment, providing sensitivity to DM as light as $\sim 500\,$MeV [90]. Every factor of 10 improvement beyond this in mass reach would require a factor of 100 improvement in energy sensitivity. New experimental concepts are thus required to probe sub-GeV DM in the near future.

In this section, we summarize proven strategies and describe the recent exciting developments in this area that include a plethora of ideas for new experimental strategies to probe DM candidates in the keV–GeV mass range. The same experiments may also be sensitive to the absorption of even lighter DM candidates, with meV–keV masses. Some techniques have already yielded constraints that are stronger by orders of magnitude than any other searches for certain DM candidates as light as a few MeV. Moreover, many techniques benefit from the on-going research and development that is already taking place to search for low-mass WIMPs and do not require a separate or new effort. Some techniques require a separate, significant effort to demonstrate their feasibility. However, it is worth noting that in many cases a modest investment of funds can allow for the required R & D.

B. General Goals and Challenges

In general, the main goals and challenges in direct detection of sub-GeV DM are:

- *Finding detectable low-threshold processes*: Sub-GeV DM has much less energy to deposit than Weak-scale DM ($\sim 1\,{\rm eV} \times (m_{\rm DM}/{\rm MeV})$). The first goal is therefore to find processes in target materials that have a low enough threshold to be triggered by light DM scattering and can potentially be detected.

- *Amplification*: Detecting these low threshold processes will typically require some amplification mechanism, which is likely to be a strong restriction on the type of process that can be considered, and may be one of the main experimental challenges.

- *Backgrounds*: The low-threshold processes to be detected should be expected to have real rates due to backgrounds. These backgrounds may be totally unrelated to the dominant backgrounds in conventional nuclear recoil searches. Indeed, in many cases the "traditional" backgrounds like cosmogenics, Compton scattering, or neutrons can be controlled and made negligible. Instead, understanding and controlling detector-specific backgrounds, often created by the amplification mechanism itself, will be among the most important challenges for any experimental design.

- *Scaling up exposure*: Some new experimental concepts may initially only be possible with very small target masses. Scaling up their size may become one of the main challenges as experiments develop.

- *Signal discrimination*: Since discovery is the primary goal of any direct detection experiment (as opposed to setting new limits), it is essential to be able to distinguish real DM scattering events from backgrounds. This may be on an event-by-event basis (such as in many of the existing nuclear-recoil DM searches) or on a statistical basis over many events (for example by annual modulation or directional sensitivity).

- *Improved material fabrication*: Some new ideas require specific target materials with, for example, unprecedented levels of purity or structural coherence. This means that advances in the technology for fabricating these materials may be necessary before such experiments are feasible.

C. Basic Strategy

While searching for nuclear recoils loses sensitivity rapidly for DM masses below a few GeV, the most fruitful strategy has been to search for DM scattering off bound electrons [19]. Scattering off an electron (as opposed to a nucleus) allows all of the available DM kinetic energy to be transferred to the bound electron. The signal depends on the material, but consists of one or more electrons (possibly amplified by an electric field) or one or more photons.

[RE: edit paragraph, add citations] For an electron with a binding energy of ΔE_B, one can in principle probe masses of

$$m_\chi \gtrsim 250 \text{ keV} \times \frac{\Delta E_B}{1 \text{ eV}} \,. \tag{17}$$

Below we review various possible materials, but we summarize them here first. **Noble liquids** provide excellent, existing target choices [19]. An ionization threshold of $\Delta E_B \sim \mathcal{O}(10 \text{ eV})$ provides sensitivity to $m_\chi \sim$ a few MeV. This was demonstrated explicitly in [91] using published XENON10 data [92] [RE: add more]. Upcoming experiments will soon have ton-year exposures, possibly providing improved sensitivity to lower scattering cross sections and the possibility to search for an annual modulation in the signal rate. **Semiconductors**, like germanium and silicon, have $\Delta E_B \sim \mathcal{O}(1 \text{ eV})$ and have potential sensitivity to $m_\chi \sim 100$'s keV to MeV [19, 93–95]. The best existing constraint on sub-GeV

DM using a silicon target [95] uses DAMIC data [96], but is orders of magnitude weaker than the XENON10 limit mentioned previously. However, the development of more sensitive detectors over the next few years could significantly improve on existing constraints. **Scintillators**, like gallium arsenide, sodium iodide, or cesium iodide, have similar or slightly larger thresholds. By searching for single photons, they could achieve sensitivity to similar masses as semiconductors [19, 97], but new efforts are required to develop the needed large-area (several cm^2) single- or few-photon detectors that can cover $\mathcal{O}(1\ \mathrm{kg})$ of material to achieve large enough exposures. **Two-dimensional targets**, like sheets of graphene, also have similar thresholds and could provide a means to distinguish signal from background by allowing for directional sensitivity to the recoiling electrons [98]. One challenge is to obtain large enough target masses ($\mathcal{O}(1\ \mathrm{kg})$), but this may be possible with the proposed PTOLEMY experiment []. **Superconductors**, like aluminum, have much lower thresholds to generate a signal ($\mathcal{O}(1\ \mathrm{meV})$) that is determined by the binding energy of a Cooper pair. This could allow for sensitivity to DM masses as light as a keV [99], the warm DM mass limit. Ultrasensitive phonon detectors requiring significant R & D over the next decade could achieve sensitivity to such low thresholds [100].

Another effort has been to suggest new techniques to probe nuclear recoils, but not with elastic recoils. Indeed, inelastic processes [19] are needed to produce measurable signals. [RE: finish] [RE: add superfluid helium [101] and chemical bond breaking].

D. Target Materials and Strategies

We now discuss some of the existing and proposed target materials, amplification mechanisms, and background reduction techniques in more detail.

Xenon-based Searches: Current Status, Challenges, and Future Prospects

Two-phase xenon-based time projection chamber (TPC) detectors have set the world-leading sensitivity [102] to DM with $m_\chi > 4$ GeV via elastic nuclear recoils, which the upcoming XENON1T and LZ experiments will improve. These experiments will also significantly improve terrestrial constraints on axion and dark-photon parameter space with $m_\chi \gtrsim 0.8$ keV via searches for DM absorption by a bound electron. The low-mass threshold on these searches is set by a large external radiogenic photon background that is shielded by the outermost layer of the active detector, and thus the DM signal must produce at least 2 measured scintillation photons (S1), so that the z-location of the event can be confirmed to be within the fiducial volume.

The smaller, previous generation of these experiments, XENON10, analyzed their data without the requirement of a measurable scintillation photon signal [92]. This data was used to set world-leading limits on the elastic scattering of DM off electrons with 5 MeV $\lesssim m_\chi \lesssim$ 1 GeV [91]. [RE: add] The dominant background for these searches was not the expected radiogenic electron recoils in the outermost shielding layer of xenon, but rather a spurious electron dark count rate. A significant but not complete fraction of this rate has been determined to be due to ionized electrons, originally created by highly ionizing background events outside of the dark matter scattering region of interest, that become trapped at the liquid-gas interface and are released spontaneously at some much later time. R&D into minimizing this source is onoing. Specifically, LZ is attempting to increase the extraction E-field at the liquid-gas interface to improve the electron transport efficiency from the ∼65% found in LUX [102] to 97.5%. More detailed analysis than completed so far may also allow many of these events to be removed as well. The large exposures possible with xenon-based

TPCs also potentially allow for for very strong annual modulation analyses.

While further research will determine the ultimate sensitivity of these experiments to sub-GeV DM, other experiments purposely designed to limit dark count backgrounds must be designed. Moreover, the ultimate mass threshold of xenon-based TPCs is $m_\chi \sim$few MeV which is set by the xenon atom's ionization energy (12.1 eV). Consequently, other detector technologies will certainly be needed to probe lower masses even under the most optimistic strategies.

Semiconductor-based and Scintillator Searches: Current Status, Challenges, and Future Prospects

CRESST [103] and SuperCDMS [104], cryogenic calorimeter based experiments with $CaWO_4$ and Ge respectively, currently lead the world in searching for elastic nuclear recoils from DM with mass from 0.5 GeV to $\sim$ 5 GeV. Both are also currently funded for next generation experiments within this mass range which should increase their sensitivity by many orders of magnitude within the next 4 years. Just as with the noble gas experiments, these experiments can be repurposed to search for electronic recoils from 1 MeV–100 MeV DM. Furthermore, since the semiconductor bandgap is over an order of magnitude smaller than the ionization energies of noble gas experiments, much lower masses could be probed.

To gain sensitivity to the small amount of ionization generated by the sub-keV nuclear recoils and very small electron recoils produced by $<$ 5 GeV DM, SuperCDMS SNOLAB drifts the e^-/h^+ pairs through the semiconducting crystal with an external E-field to convert their electrostatic potential energy into measureable athermal phonon energy that can be collected and measured with sensors fabricated onto the surface of the detector. The dominant potential disadvantage of using this phonon amplification technique is that the semi-conducting crystal is fundamentally out of equilibrium, and thus any tunnelling or IR photon excited process that allows an e^- to transport across the crystal would produce a dark current, which could limit the sensitivity, in a similar way to that seen in xenon TPCs. Over the next 2 years, SuperCDMS plans on studying a variety of insulating surface layers and plans on improving their phonon sensor sensitivity such that E-fields as low as 10 V/cm can be used to drift the ionization (x100 less than the E-fields used in Xenon TPCs).

If the dark count rate can not be minimized in non-equilibrium semiconductor detectors, then one must design an experiment in which the large active detector volume is in equilibrium (no intrinsic amplification), but which still has sensitivity to single electronic excitation. One strategy is to measure electronic recoils from DM in direct bandgap semiconductors (GaAs) and other relatively low bandgap scintillators (NaI, CsI) without the use of external E-fields via measurement of scintillation photon production [97]. Of course, the large area photon detectors used must also have negligible dark counts (no PMTs). One promising pathway is to build detectors from mKID and TES superconducting technology (which should by nature be dark-count free), and within the next 2 years it is hoped that athermal phonon technology from SuperCDMS could be repurposed. An additional potential advantage over traditional SuperCDMS technology is that the separation of the active absorber volume from the sensor means that cosmogenic backgrounds like ^3H can be drastically reduced, because the crystals can be stored underground for their entire lifetime.

Two other potential challenges for this technique is to find scintillators for which the scintillation photon production is $\mathcal{O}(1)$ and for which the afterglow (excitations tunneling off of crystal impurities) rate is non-existent. For example, if a crystal cannot be found with an afterglow rate $<$ 10 events/kg/yr, then it's been proposed that either optical filters or a photon sensor with the capability to distinguish near bandgap excitation scintillation from

photons due to deep level crystal impurities could be used to distinguish DM recoils from afterglow photons.

Other Materials

Superfluid ^{4}He has both long-lived vibrational excitations with energies $\sim$ 1 meV as well as long lived electronic excitations with energy near $\sim$18 eV (ionization, EUV singlet scintillation photons, and metastable triplet excimers). As such, a high detection efficiency for these varied excitations would enable a detector sensitive to low-energy electronic and nuclear recoils from DM scattering.

Scintillation light from both singlet and triplet states could be collected and measured with cryogenic large area single photon sensitive detectors similar to those proposed for crystal scintillator DM experiments. Direct measurement of the ionization could be possible using a standard 2 phase TPC detector configuration. However, the mobility of e^- in He is much less than seen in other noble liquids. Consequently, very high E-fields would be necessary, which may lead to a significant dark count rate. Finally, rotons and other athermal phonon vibrations naturally eject He atoms when they hit a liquid/vacuum interface. HERON showed that these ejected atoms could then be adsorbed onto the surface of a large area calorimeter hung above the superfluid for measurement. Importantly, this process has natural amplification, since the attraction potential of the He atom to the surface is an order of magnitude larger than vibrational energies themselves.

In the DM mass range from 100 MeV to 10 GeV, kinetic energy is transferred from the DM to the $\sim$ 4 GeV ^{4}He nuclei extremely efficiently compared to Si and Ge. Consequently, electron recoil / nuclear recoil discrimination of radioactive backgrounds could be feasible down to very low masses even though the ionization energy scale is an order of magnitude larger than those found in Ge and Si. On the otherhand, the small mass means that the coherent scattering rate enhancement is much smaller for He than Ge and Si. A second clear advantage of He in this mass range compared to Ge and Si is that the long-lived radiogenic ^{3}H background produced by cosmic ray spallation that is believed to be the dominant background for SuperCDMS SNOLAB experiment can be easily removed through distillation.

Due to the large electronic excitation energy, ^{4}He is unfortunately not the preferred target material for searching for electronic recoils from DM with mass in the range of 1 MeV- 50 MeV.

In [101], it was proposed to use off-shell elastic scattering processes, whereby DM could produce two nearly back-to-back helium jets that carry large fractions of the DM kinetic energy. If detection is feasible, ultra sensitive superfluid He detectors could be sensitive down to the keV warm DM limit.

The use of superconducting calorimeters has also been proposed to extend the sensitivity of direct detection down to the warm DM limit. Compared to liquid He, the calorimeter sensitivity requirements are over an order of magnitude more severe due to the lack of amplification. On the other hand, the scattering rates themselves are tree level.

[RE: add summary of molecular targets, color centers, carbon nanotubes, ...]

E. Distinguishing Signal from Background

Several suggestions exist to distinguish signals from backgrounds. First, it should be emphasized that the DM-induced electron recoil spectrum is expected to look rather distinct from that of background events. But several additional handles exist. The classic signal is to

search for an annual modulation of the event rate induced by the motion of the Earth around the Sun [105]. Since most processes under consideration are inelastic (e.g., scattering off a bound electron), the expected modulation amplitude is larger than that for elastic nuclear recoils. This amplitude also has a distinct dependence on threshold energy, and is unlikely to be mimicked by a modulating background. Another possibility is to use 2D materials (like graphene) to detect the directionality of the recoiling-electron event [98]. Gravitational focusing of DM by the Sun also induces interesting modulation effects [94]. Also, it was proposed to use the inherent asymmetries in crystals to search for a daily modulation of the event rate.

F. Overview of Models

As already emphasized in the introduction and the other sections of this report, there are many well motivated DM candidates in the keV–GeV mass range. In particular, direct detection can probe DM models that couple to electrons and/or nucleons through a light mediator (mass $\lesssim$ GeV), as long as the scattering is elastic or very-nearly elastic. Moreover, direct detection is by far the most sensitive probe of models with an ultralight mediator (mass $\ll$ keV). Such a light mediator enhances the rates for low momentum-transfer events (relevant for direct detection) compared to high momentum-transfer events (relevant for collider or fixed-target searches). The canonical mediator possibilities are a dark photon, but also the photon (e.g. DM with an electromagnetic dipole moment). Other possibilities exist.

Even lighter bosonic DM candidates may be detectable with the same experimental setups if they can be directly absorbed. Axion-like pseudoscalar DM or hidden-photon-like vector DM are the most natural examples.

As a rule of thumb, the lighter the DM candidate, the more stringent the astrophysical and cosmological bounds it must evade. These include CMB distortions due to late DM annihilations (for $m_{\rm DM} \lesssim 10\,{\rm GeV}$), changes to $N_{\rm eff}$ measured from the CMB (for $m_{\rm DM} \lesssim 10\,{\rm MeV}$), SN 1987a cooling (for $m_{\rm DM} \lesssim 10\,{\rm MeV}$), stellar/white dwarf cooling (for $m_{\rm DM} \lesssim 10\,{\rm keV}$), solar cooling (for $m_{\rm DM} \lesssim 1\,{\rm keV}$). Nevertheless, there are many sub-GeV DM candidates which evade all known bounds, have a potential productional mechanism, and which may be discoverable with new direct detection experiments.

Certain models, particularly those with a hidden-photon mediator in the MeV–GeV mass range, may be discoverable both with the direct detection experiments discussed in this section, and with the beam-dump / collider experiments discussed elsewhere in this report. Other models, particularly those with a much lighter mediator, are likely to be discoverable only with direct detection experiments.

In Fig. 11 we show examples of models with DM coupling to a heavy dark photon ($m_{A'} \sim m_\chi$) and an ultralight dark photon ($m_{A'} \ll m_\chi$). In Fig. **??** we show the reach of these experiments for DM absorption. [RE: describe; explain mapping of y to $\overline{\sigma}_e$; maybe add absorption plot]

Further details and discussion can be found, for example, in Refs. [19, 93, 95, 100, 106–108].

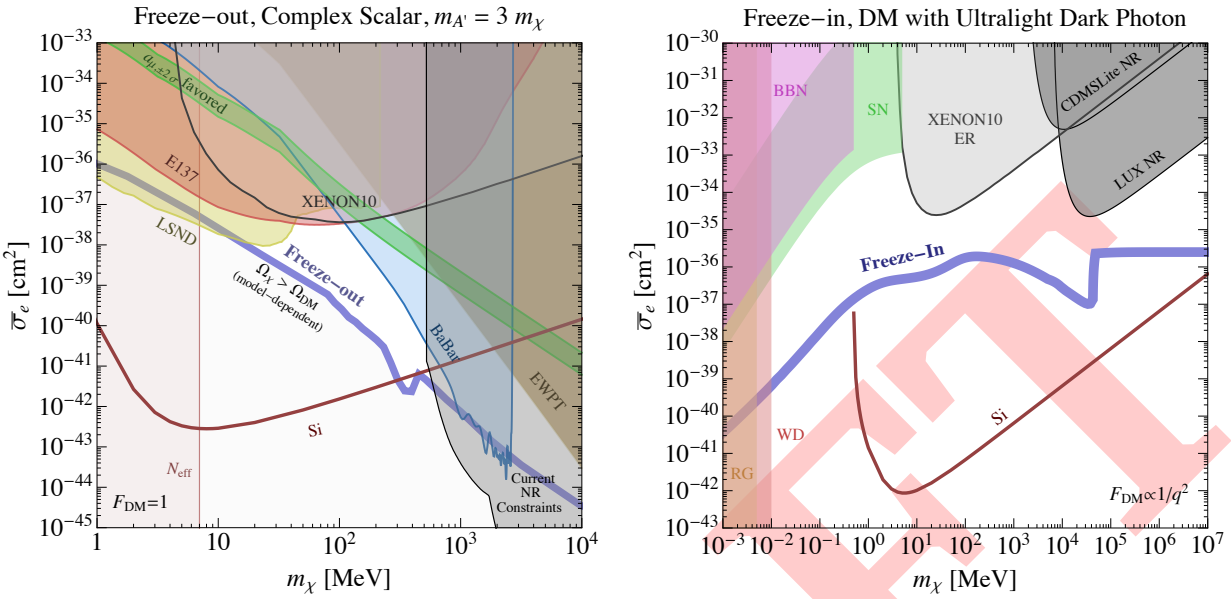

FIG. 11: **Event Rates for Various Materials [RE: placeholder plots]** [RE: add scintillators, superconductors, graphene etc.]

G. Outlook

While xenon-based experiments have demonstrated sensitivity to DM down to masses of a few MeV and further research is needed before their ultimate sensitivity is known, the large dark-count rate makes it highly desirable to use other techniques and materials. Over the next few years, the potential of semiconductors will be better quantified. In particular, the dark-count rate in semiconductors using Luke-Neganov gain must be quantified to determine if they provide the best path forward. Large-area single-photon sensitive detectors must be developed for Superfluid He and scintillating-crystals experiments, and the next few years may see significant progress in this arena. Other techniques, including the use of 2D targets, color centers, and superconductors will continue to be developed on a longer time-scale. The multitude of ideas suggests a healthy field from which much progress can be expected over the next 5–10 years.

VI. RICH DARK SECTORS

Convenors: Bertrand Echenard, David E. Morrissey, Brian Shuve. Organizer Contact: Matt Graham

A. Introduction

The physics of the Standard Model (SM) is complex: there are multiple non-gravitational forces, mass scales originate both from dimensionful parameters of the theory and via dimensional transmutation, and the origins of flavor and CP violation are unknown. Furthermore, the SM is just the tip of the iceberg: it comprises only 15% of the matter in the universe, and identifying the composition and nature of the remaining dark matter (DM) is one of the major outstanding problems in particle physics. While DM could be just a single new particle, it may also arise as part of an entire dark sector containing many new particles and forces. There is no reason for such a dark sector to be substantially simpler than the visible matter of the SM.

When DM is part of a larger dark sector, its experimental signatures can differ substantially from minimal DM scenarios, such as those of a Weakly Interacting Massive Particle (WIMP). The complementarity of different experiments in probing the DM parameter space, as well as the range of parameters motivated by cosmology and astrophysics, are also more complicated in DM models with dark sectors. While minimal models offer simple motivations for many DM searches, it is possible that some striking signatures of DM physics would be missed with the current program that focuses primarily on WIMPs. Indeed, much of the rich phenomenology observed in the SM is independent of the physics establishing the cosmological abundance of protons and electrons. Given the lack of any positive detection of DM to date, it is imperative to broaden our search strategies to allow a discovery over as wide a range of theories as possible. Conversely, should a DM signal be observed, a thorough exploration of the dark sector would be required.

Dark sectors with a characteristic mass below the electroweak scale have been the subject of recent interest [12]. This possibility was motivated by putative astrophysical observations of DM annihilation that suggested the presence of a new, light gauge boson that mediates interactions between the SM and DM [109, 110], typically referred to as a "dark photon". New experimental programs dedicated to the discovery of such dark photons in their visible and invisible decays were established soon after [111], and such experiments are the focus of earlier sections in this report.

Even in such a simple scenario, however, many questions arise. What is the origin of the mass of the dark gauge boson? Does it have its own Higgs mechanism, and if so, does this induce a new hierarchy problem? Are there any states in the dark sector beyond the DM particle and the dark photon, and how do these states influence the cosmology and phenomenology? Is there strong dynamics in the hidden sector? Are the couplings of the new dark states different from those assumed in the minimal dark photon model, and is there a way to ensure a comprehensive experimental program for discovering all of the dark sector states? These questions, among others, motivate the study of so-called "rich dark sectors". The goal of this working group is to identify the challenges and opportunities in expanding our sensitivity to a wide range of dark sector models beyond just the minimal dark sector scenario.

B. Exploring Rich Dark Sectors

A major challenge in studying rich dark sectors is the large number of possible particles and couplings. In this workshop, we focused on three broad categories to provide an organizational framework for discussing experimental signatures and identifying areas for future development. The categories are: *dark-sector masses and naturalness*, which focused on models explaining the origin of dark-sector masses or their naturalness, and potential connections with the SM Higgs mechanism; *non-minimal dark matter*, which highlighted theories where DM has non-standard interactions and examined the consequent astrophysical, cosmological, and experimental implications; and *exotic dark sectors*, which studied an array of models extending the minimal dark photon paradigm.

1. *Dark-Sector Masses and Naturalness*

Dark sectors with massive vector, fermion, and scalar fermion degrees of freedom naïvely raise many of the same questions as the SM: what sets the masses of the dark states, and is the hierarchy between the dark sector masses and the Planck scale natural? For dark sectors with masses at or below the weak scale, it is reasonable to consider whether the dark masses are set by an independent Higgs mechanism, a Stueckelberg mechanism if the gauge symmetry is Abelian, or some extended symmetry breaking that is shared amongst the visible and dark sectors. In most models accounting for dark sector masses, new states are required beyond a single DM candidate or a dark force mediator, and this leads to new experimental constraints and possibilities.

One of the simplest mechanisms of dark mass generation is a dark Higgs field. The corresponding dark Higgs boson h' can be produced in the dark Higgs-strahlung process, $A'^* \to A'h'$, where A' is the massive dark gauge boson connected to the SM through the vector portal [112, 113]. Such a process can occur wherever dark gauge bosons are produced, such as in B factories, proton colliders, and fixed-target experiments. The experimental signals of this process depend on how the dark Higgs h' decays. When $M_{h'} \gtrsim M_{A'}$, the dominant decay is $h' \to A'A'^{(*)}$, which can give rise to multi-lepton (or multi-pion) final states [112]. Such signatures have been the subject of searches at *BABAR* and Belle and are nearly background free [36, 114], suggesting that Belle II should have very good sensitivity. If $M_{h'} < M_{A'}$, the h' decays through a loop of A' vectors to a pair of SM states [112], or by its mixing with the SM Higgs [115]. For both such h' decay modes, the decay rate receives a strong suppression, from two factors of the kinetic mixing in the former and the small SM Yukawa couplings in the latter, often leading to displaced or invisible decays [112].

Dark sectors with fundamental scalars can suffer from a hierarchy problem, and models which alleviate their fine tuning generally predict additional states connected with the dark Higgs sector. As a concrete example, supersymmetric theories with a dark photon and Higgs predict additional dark gaugino and Higgsino states [116–118]. Searches at ATLAS and CMS for dark photons produced in SM Higgs decay are sensitive to some of these scenarios by looking for lepton jets, highly collimated collections of leptons [119, 120]. New dark supersymmetric (SUSY) states can also be produced in dark photon decays and give rise to additional new signals. For example, if the dark photon decays to the lightest and next-to-lightest dark neutralinos, $A' \to \chi_1^x \chi_2^x$, the heavier dark neutralino χ_2^x often has a long lifetime and can be seen in fixed-target/beam-dump experiments, as well as in displaced vertex searches at B factories and hadron colliders [9][200]. Such signatures are not completely

covered in existing experimental analyses.

Even more exotic signatures are possible when the dark photon is part of an extended non-Abelian gauge sector [121], or if the breaking of the gauge symmetry is due to strong dynamics [113, 122, 123]. In the latter scenarios, the mass scale is natural in the same manner as the proton mass in Quantum Chromodynamics (QCD). The resulting spectrum of states is very rich and is similar to that found in Hidden Valley models [124]. Many Hidden Valley signatures have been proposed over the years, including long-lived decays [125], emerging jets [126], and semi-visible jets [127]. Many of these possibilities have not yet been directly studied at low-energy experiments.

2. Non-Minimal Dark Matter

Cosmological and astrophysical observations of DM can be largely explained by a cold (non-relativistic), collisionless DM particle [128]. However, a variety of studies of small-scale structure over the past two decades have uncovered conflicts between the predictions of cold dark matter (CDM) simulations and the observed DM halo profiles and distributions [129–131]. Recent simulations of structure formation that include the effects of baryonic feedback on DM halos give better agreement with observations, but it is an open topic of debate whether this can account for all of the discrepancies [132–135]. If the disagreements between simulations and observations persist, this may give evidence for new physics beyond collisionless DM, such as DM with self interactions.

The cross sections needed to resolve the small-scale structure anomalies ($\sigma/M_{\rm DM} \sim 1\,{\rm cm}^2/{\rm g}$) are much larger than a typical electroweak scattering rate [136–138], and can be challenging to realize in models of DM that are consistent with other constraints on interacting DM such as from the Bullet Cluster [139–141]. In models of self-interacting dark matter (SIDM), where DM interacts with itself via a light mediator, the velocity dependence of the cross section can render SIDM consistent with all current constraints [142], and observations of small-scale structure may even allow for the determination of the DM and mediator masses without any direct interactions with SM fields [143].

The SIDM paradigm provides an additional astrophysical motivation for light mediators within the dark sector. However, the coupling of the mediator to SM fields can be much smaller in these models than is accessible in standard dark photon or Higgs searches. Such tiny couplings may be tested by precision probes of Big Bang Nucleosynthesis (BBN) and the Cosmic Microwave Background (CMB), as late decays of the mediator can disrupt the standard cosmology [144, 145].

Large dark scattering rates mediated by new light dark forces can also lead to the formation of DM bound states [122, 146–148]. Such bound states can then decay via annihilation of the constituent DM particles, giving an alternative mechanism for DM indirect detection. Indeed, the formation of bound states can dominate over the Sommerfeld enhancement that is typically considered in the annihilation of interacting DM [149]. Bound states of DM can also be produced in B factories and high-energy colliders, leading to striking decays to multi-mediator final states [148, 150]. Experimental searches for the full range of these signals remain to be performed at both low- and high-energy colliders.

Finally, non-minimal DM scenarios can dramatically change the nature of DM signals in various experiments. For example, the presence of strong DM self-interactions can lead to a radically different evolution of the DM abundance due to cannibalization and $3 \to 2$ scattering [151], such as in SIMP [152] or ELDER [153] models. These mechanisms are typ-

ically realized for DM candidates that are qualitatively different from conventional WIMPs. There are also non-thermal scenarios that, once again, break the relation between couplings and masses found in WIMP models [154]. An intriguing example of a non-thermally established DM abundance are models of asymmetric DM, where the DM abundance arises from a dark matter-antimatter asymmetry [155]. If this asymmetry is connected with baryon- or lepton-number-violation in the visible sector, then DM can lead to dramatic signatures such as induced nucleon decay [156]. Finally, the DM halo structure can be different in extended dark sectors relative to collisionless WIMP models, leading to different predictions for direct- and indirect-detection experiments. Non-minimal DM models clearly motivate a wide array of non-traditional searches for dark-sector states and forces.

3. Exotic Dark Sectors

Exotic dark sectors encompass any model that extends beyond the minimal vector, Higgs, or neutrino portals. Such sectors frequently lead to (optimal) search strategies that are not included in the current dark-sector discovery program. These theories can be motivated by various anomalies such as the excess in muon $(g-2)_\mu$ [157], the puzzle of the proton charge radius [158], as well as hints of new particles in beryllium nuclear transitions [159]. Exotic models are also motivated by many of the mass and DM considerations discussed above. An overarching theme of the workshop discussions was that the related "exotic signatures" do not necessarily arise from complicated or contrived hidden sectors. For instance, a single new light mediator with large couplings to DM can lead to the formation of DM bound states that qualitatively change the phenomenology of the hidden sector [122, 146–148].

In other examples, new light scalars or vectors could be hidden from existing experiments if their couplings differ from the predictions of the minimal dark-photon or dark-Higgs scenarios. For example, if SM fields are charged directly under the gauge interaction of a new hidden sector, the couplings can be very different from a kinetically mixed dark photon: $B-L$ interactions would lead to new couplings between neutrinos, leptons, and nucleons [160], while an $L_\mu - L_\tau$ gauge interaction would decouple the new gauge boson from the initial states of low-energy electron accelerator experiments [161]. Similarly, a scalar coupling via mixing with an extended electroweak symmetry breaking sector can give scalars with enhanced couplings to heavy-flavor leptons and suppressed couplings to electrons and quarks [162, 163]. Finally, a protophobic force could account for the recently hypothesized new particle produced in $^8\mathrm{Be}^*$ decays while remaining consistent with dark-photon bounds [164].

It is challenging to comprehensively explore exotic dark signatures with existing or new experiments. The Search for Hidden Particles (SHiP) Experiment, a proposal to build a particle detector 50 m downstream from the beam dump of the Super Proton Synchrotron (SPS) at CERN [43, 71], could provide sensitivity to a wide variety of models with long-lived particles. Since most models connecting dark forces to the SM will induce couplings to nucleons via higher-order processes, SHiP would be an excellent model-independent probe of exotic new physics. In background-limited environments such as the LHC or B factories, it is possible to design targeted searches for well-motivated exotic signatures that give excellent sensitivity. Existing experiments such as SeaQuest can also be re-purposed with electron and pion reconstruction abilities to enhance the prospects for exotic signature discoveries [165]. Finally, dedicated experiments may be needed to probe new particles that would not register in any other experiment; a recent example is the MilliQan proposal at the LHC to search for

new milli-charged particles [166]. Opportunities to implement relatively low cost, parasitic experiments at existing facilities should be explored further.

C. Synthesis and Summary

While each discussion focused on different aspects of rich dark sectors, several common themes emerged from the presentations, questions, and conversations. It is impossible to design experimental and theoretical programs that are able to probe every possible DM model; however, the proposals below are meant to expand sensitivity to as many rich dark sector scenarios as possible. While this should not come at the expense of searches for the canonical kinetically-mixed dark photon models, small variations in experimental or analysis strategies could broaden the spectrum of final states that can be discovered at each experiment.

1. **Existing or planned experiments can be sensitive to rich dark sectors.**
   It is not necessary to reinvent every search and experiment! For example, in dark photon scenarios with a large dark gauge coupling leading to the formation of DM bound states, existing searches for visibly-decaying dark photons can also be sensitive to invisibly decaying dark photons followed by bound-state decay [148]. Similarly, constraints on kinetically-mixed dark photons can easily be mapped into the parameter spaces of new gauge interactions like $B-L$ or L_e-L_μ. Existing experiments designed for other purposes could also have sensitivity to new dark states. For example, neutrino beam experiments are sensitive to $L_\mu-L_\tau$ interactions via the neutrino trident process [161], while neutrino detectors could serve as "direct detection" experiments for boosted DM coming from the Galactic Center or the Sun [167–169].

   To facilitate the reinterpretation of existing results, experiments should provide as much information as possible about the specific couplings that are driving their limits (or discoveries). Such results can be made more transparent by, for example, reporting constraints from dark photon searches as a function of individual couplings to e, μ, q (or products thereof) in addition to the $M_{A'} - \epsilon$ parameter space. To illustrate how experimental sensitivities can change in an exotic dark sector, we show in Fig. 12 the constraints on a boson that couples mass-proportionally to leptons [163]; the constraints are very different than for a kinetically mixed dark photon (see Sec. **??**). Also, experiments should consider how minor additions or modifications to their trigger and reconstruction strategies could be used to ensure sensitivity to harder-to-reach dark sector scenarios. In conjunction with these experimental efforts, theorists should develop a set of simplified models that capture a broad range of behaviors of rich dark sectors to facilitate such planning.

2. **Dedicated rich dark sector searches are also needed.**
   Many signals predicted by rich dark sectors do not arise in more minimal models. However, the number of possible signals is nearly limitless. Theoretical guidance will be important to select the most promising search directions, but it is also essential that experimental proposals be designed to be sensitive to as wide a range of models as possible. As an example, consider searches for six-lepton final states at B-factories [36, 114]. These can arise both by Higgs-strahlung, $e^+e^- \to A'h', h' \to A'A'$ with $A' \to \ell^+\ell^-$ [112], as well as from the direct production and decays of dark bound states,

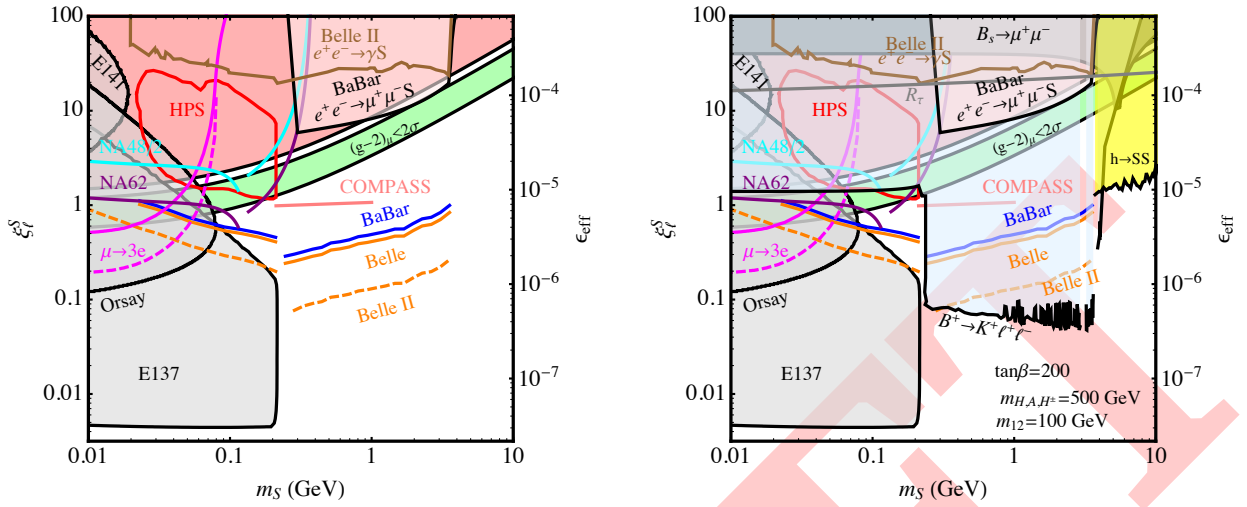

FIG. 12: Constraints on a leptophilic scalar S from Ref. [163]; the scalar coupling to each lepton ℓ is equal to ξ_ℓ^S times the SM Yukawa coupling for ℓ. *Left:* Model-independent limits and projections assuming only the coupling of S to leptons. *Right:* Limits and projections for a UV-complete model that leads to additional couplings between S and b quarks (see Ref. [163] for details).

$\Upsilon_{\rm D} \to A'A'A'$, $A' \to \ell^+\ell^-$ [148]. By expanding the selection requirements of these searches to include events where the total final-state energy does not reconstruct the beam energy, they could also be sensitive to more general dark sector processes with some invisible particles in the final state.

A useful guide for organizing dark-sector experimental channels can be found in SUSY multi-lepton searches at the LHC [170, 171]. These searches are organized in signal regions of different lepton flavors, associated jet multiplicities, b-jets, and so forth; although theory models rarely predict signatures that populate a single bin, the background estimates and event counts in each bin give sensitivity to many models beyond those officially studied in the analysis. Where appropriate, organizing searches at low-energy experiments in a similar fashion could greatly enhance their ranges of applicability.

3. **Communication between theorists and experimentalists is key.**
In many cases, experiments are capable of performing various searches without knowing whether any theoretical motivations exist, while theorists are not necessarily aware of all of the opportunities and limitations of each experiment. This problem will only intensify with a proliferation of new experiments and renewed theoretical interest in dark sectors. An online repository or forum that collects experimental and theoretical ideas, classified by signature, could be a helpful resource to promote more fruitful interactions between theorists and experimentalists, as well as to reduce redundancy in efforts among researchers in the field.

   For such an effort to be successful, theorists would have to provide Monte Carlo (MC) tools and events for use by experimentalists. In return, experimentalists should work to report results in as model-independent a manner as possible. For example, approximate publicly available parameterizations of reconstruction efficiencies, detector geometries, and fiducial cross section limits have been very useful in broadening the

applicability of searches for new physics at high-energy colliders[201]. Given the nature of low-energy experiments, it may not be possible to provide some or all of this information for a given experiment, but a description that allows even a rough estimate of sensitivity can be helpful to theorists for determining whether an experiment could have any sensitivity to a given model.

4. **Complementarity is complicated.**
One of the most appealing aspects of accelerator-based studies of DM is their complementarity to cosmological, astrophysical, and direct-detection probes of DM. However, the crossing symmetry relating these various search strategies applies strictly only to minimal DM candidates. In rich dark sectors, the connections between different experiments might be broken. In light of the complexity of possible signatures, it is imperative that experimental results be stated as precisely as possible (both by theorists and experimentalists), with all caveats clearly identified. For example, explanations for the muon $(g-2)$ anomaly or the putative ^{8}Be signal based on minimal dark photons are ruled out by direct dark photon searches, but allowed in variants of the minimal model with a slightly more complicated coupling structure. In a concrete model, it is possible to apply experimental searches for different signatures to the same parameter space: for example, in a model with a dark photon and multiple dark states, it is possible in certain limits to combine experimental results from LHC lepton-jet searches with canonical dark photon searches. An example of this is given in Fig. 13, that shows the current sensitivity of the ATLAS and CMS experiments to a specific scenario in which dark photons are produced in the decays of the SM Higgs boson. The LHC searches cover a large region of the model space that is inaccessible to lower-energy probes.

   With extended rich dark sectors, a whole host of new constraints can also arise that are absent in minimal models. New forces coupled to neutrinos could face formidable bounds from neutrino scattering constraints, while sufficiently long-lived particles can unacceptably modify the predictions from various cosmological epochs. Since every ground-based, astrophysical, and cosmological search for new physics could, in principle, have sensitivity to dark sector models, a repository as proposed above would be useful in ensuring that all proposed models are consistent with existing constraints.

5. **New tools may be needed.**
Given the plethora of existing bounds on dark sectors, as well as the challenge of MC simulation for some low-energy experiments, developing a framework for automating Monte Carlo (MC) event generation and limit setting would be invaluable. Tools such as `MadDM` exist that take generic models in `UFO` format and compute various experimental rates and properties of interest [172, 173]. However, many of these tools are very WIMP focused, and an extension to low-mass DM would be needed. A framework which allows users to write modules to automate the computation of relic abundances of light thermal DM, non-thermal DM, asymmetric DM, and other non-WIMP scenarios, as well as a whole host of cosmological and astrophysical bounds, would be desirable; this would minimize redundant computations and ensure more accurate automated results across a broad range of rich dark sector scenarios.

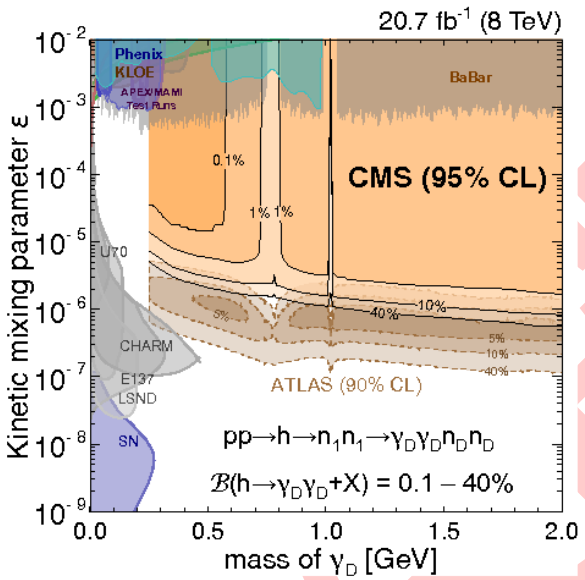

FIG. 13: Constraints on a dark-sector SUSY model with a dark photon and multiple dark states (combination from Ref. [120]). ATLAS and CMS constrain production of the dark matter through the Higgs portal and subsequent decays, while other experiments directly constrain the dark photons.

Appendix: Summary of Current Experiments

- **B- and ϕ-Factories**
  In the past two decades, high-luminosity e^+e^- collider experiments such as *BABAR* Belle, and KLOE were conducted with collisions tuned to the energies of various hadronic resonances. The low center-of-mass energies and large data sets give these experiments excellent sensitivity to low-mass dark sectors. KLOE II is now taking data and Belle II will come online in a few years to further improve sensitivity.

  Complementing the searches for standard visibly and invisibly decaying dark photons, *BABAR* and Belle have searches for dark Higgs production via Higgs-strahlung, $e^+e^- \to A'h'$, $h' \to A'A'$ [36, 114], while KLOE searched for the same process with invisible dark Higgs decays [42]. *BABAR* additionally studied a scenario where the dark photon is embedded in a dark non-Abelian gauge group via the reaction $e^+e^- \to A'^* \to W'W' \to 4\ell$ [174]. Finally, *BABAR* recently performed a model-independent search for a boson coupled exclusively to muons via $e^+e^- \to \mu^+\mu^- Z'$, $Z' \to \mu^+\mu^-$ [175],

providing a test of $L_\mu - L_\tau$ gauge bosons and leptophilic scalar scenarios above the dimuon threshold. *BABAR* is currently searching for a dark scalar boson S in $e^+e^- \to \tau^+\tau^- S, S \to \mu^+\mu^-, e^+e^-$, as well as self-interacting dark matter in 6 lepton final states.

- **High-Energy Colliders**
  Low-mass dark sectors can be challenging to discover at high energy colliders because the characteristic energy of dark-sector processes is small compared with the collision energy. If, however, dark-sector states are predominantly produced through the decays of heavy particles such as gauge or Higgs bosons, as is the case in many rich dark sectors, then high-energy colliders provide the best sensitivity to dark-sector physics. The new dark particles are typically produced in the boosted regime, leading to distinctive signatures. ATLAS, CMS, and LHCb each have growing search programs for RDS physics.

  ATLAS results include searches for pairs of both displaced and prompt lepton jets [119, 176], which are interpreted in terms of a model with Higgs decays into a hidden sector; searches for new low-mass, long-lived, hadronically decaying particles predicted in various Hidden Valley and other dark-sector models [177, 178]; searches for new dilepton resonances produced in Higgs decays [179, 180]; and searches for new low-mass diphoton resonances [181] or hidden-sector particles decaying to photons and dark matter [182].

  CMS results include a search for pairs of muon jets [120]; searches for new low-mass, long-lived, leptonically or hadronically decaying particles [183, 184]; searches for Higgs decays to new dark-sector particles, including dilepton and b-quark resonances [185–187]; and a search for exotic Higgs decays to low-mass dark matter and photons [188].

  As a forward detector dedicated to the study of heavy-flavor physics, LHCb has a relatively high trigger efficiency and acceptance for low-mass particles, and its excellent vertexing capabilities allow it to perform sensitive searches for long-lived particles. However, LHCb has a much lower integrated luminosity than ATLAS or CMS. LHCb results include a search for new low-mass, long-lived, hadronically decaying particles [189]; a search for new leptonic resonances in $B \to K^* \mu^+ \mu^-$ [45]; and searches for new lepton-number-violating sterile neutrinos [190, 191].

  MilliQan is a proposal to search for milli-charged particles produced in pp collisions at the LHC with an increased sensitivity in the 1–100 GeV mass range compared to current bounds.

- **Beam Dump Experiments**
  Rich dark sectors frequently contain new light, long-lived states. In beam dump experiments, such particles can be created from collisions in the primary target and detected through their scattering or decays in the downstream detector. Signals from scattering are typically very similar to those discussed in Section **??**, but a new possibility in RDS models is the decay of long-lived states in the beam dump detector. This was used in Refs. [9, 63, 167] to derive limits on RDS theories with a dark photon that decays primarily to long-lived dark Higgs scalars or fermions using data from CHARM [192], E137 [193], with future improvements expected from BDX [73] and SHiP [71]. Beam dumps can also be used to probe dark sectors with light vectors that couple to visible matter more generally than just gauge kinetic mixing. For example,

the observed rates of neutrino trident scattering in CHARM-II [194] and CCFR [195] were used in Ref. [196] to place bounds on a new $L_\mu - L_\tau$ force.

- **Nuclear Decays** Detailed measurements of nuclear transitions offer a further probe into light dark sectors. A recent example is the distribution of opening angles between e^+e^- pairs emitted in the decay of an 18 MeV excited state of ^{8}Be down to the ground state [159]. The observed distribution shows an excess at large angles, and can explained by the existence of a protophobic dark force [164].

[1] e.g. https://confluence.slac.stanford.edu/display/hpsg/.
[2] C. Bird, R. V. Kowalewski, and M. Pospelov, Mod. Phys. Lett. **A21**, 457 (2006), hep-ph/0601090.
[3] G. Krnjaic (2015), 1512.04119.
[4] S. Dodelson and L. M. Widrow, Phys. Rev. Lett. **72**, 17 (1994), hep-ph/9303287.
[5] F. F. Deppisch, P. S. Bhupal Dev, and A. Pilaftsis, New J. Phys. **17**, 075019 (2015), 1502.06541.
[6] K. A. Olive et al. (Particle Data Group), Chin. Phys. **C38**, 090001 (2014).
[7] B. Holdom, Phys. Lett. **B166**, 196 (1986).
[8] E. Izaguirre, G. Krnjaic, and B. Shuve, Phys. Rev. **D93**, 063523 (2016), 1508.03050.
[9] D. E. Morrissey and A. P. Spray, JHEP **06**, 083 (2014), 1402.4817.
[10] J. Jaeckel and A. Ringwald, Ann. Rev. Nucl. Part. Sci. **60**, 405 (2010), 1002.0329.
[11] *Fundamental Physics at the Intensity Frontier* (2012), 1205.2671, URL `http://inspirehep.net/record/1114323/files/arXiv:1205.2671.pdf`.
[12] R. Essig et al., in *Community Summer Study 2013: Snowmass on the Mississippi (CSS2013) Minneapolis, MN, USA, July 29-August 6, 2013* (2013), 1311.0029, URL `https://inspirehep.net/record/1263039/files/arXiv:1311.0029.pdf`.
[13] D. Tucker-Smith and N. Weiner, Phys. Rev. **D64**, 043502 (2001), hep-ph/0101138.
[14] M. Pospelov, Phys. Rev. **D80**, 095002 (2009), 0811.1030.
[15] S. Dimopoulos and H. Georgi, Nucl. Phys. **B193**, 150 (1981).
[16] F. del Aguila, G. D. Coughlan, and M. Quiros, Nucl. Phys. **B307**, 633 (1988), [Erratum: Nucl. Phys.B312,751(1989)].
[17] M. Pospelov, A. Ritz, and M. B. Voloshin, Phys. Lett. **B662**, 53 (2008), 0711.4866.
[18] L. J. Hall, K. Jedamzik, J. March-Russell, and S. M. West, JHEP **03**, 080 (2010), 0911.1120.
[19] R. Essig, J. Mardon, and T. Volansky, Phys. Rev. **D85**, 076007 (2012), 1108.5383.
[20] X. Chu, T. Hambye, and M. H. G. Tytgat, JCAP **1205**, 034 (2012), 1112.0493.
[21] G. W. Bennett et al. (Muon g-2), Phys. Rev. **D73**, 072003 (2006), hep-ex/0602035.
[22] P. J. Mohr, B. N. Taylor, and D. B. Newell, Reviews of Modern Physics **84**, 1527 (2012), 1203.5425.
[23] J. R. Batley et al. (NA48/2), Phys. Lett. **B746**, 178 (2015), 1504.00607.
[24] J. Liu, N. Weiner, and W. Xue, JHEP **08**, 050 (2015), 1412.1485.
[25] S. Abrahamyan et al. (APEX), Phys. Rev. Lett. **107**, 191804 (2011), 1108.2750.
[26] R. Essig, P. Schuster, N. Toro, and B. Wojtsekhowski, JHEP **02**, 009 (2011), 1001.2557.
[27] H. Merkel et al. (A1), Phys. Rev. Lett. **106**, 251802 (2011), 1101.4091.
[28] H. Merkel et al., Phys. Rev. Lett. **112**, 221802 (2014), 1404.5502.
[29] M. Battaglieri et al., Nucl. Instrum. Meth. **A777**, 91 (2015), 1406.6115.
[30] J. Balewski et al., in *Community Summer Study 2013: Snowmass on the Mississippi (CSS2013) Minneapolis, MN, USA, July 29-August 6, 2013* (2013), 1307.4432, URL `https://misportal.jlab.org/ul/publications/view_pub.cfm?pub_id=12467`.
[31] J. Balewski et al. (2014), 1412.4717, URL `http://inspirehep.net/record/1334361/files/arXiv:1412.4717.pdf`.
[32] *The Cornell-BNL FFAG-ERL Test Accelerator: White Paper*, `https://arxiv.org/abs/1504.00588`.

[33] B. Wojtsekhowski, AIP Conf. Proc. **1160**, 149 (2009), 0906.5265.
[34] B. Wojtsekhowski, D. Nikolenko, and I. Rachek (2012), 1207.5089.
[35] M. Raggi, V. Kozhuharov, and P. Valente, EPJ Web Conf. **96**, 01025 (2015), 1501.01867.
[36] I. Jaegle (Belle), Phys. Rev. Lett. **114**, 211801 (2015), 1502.00084.
[37] F. Archilli et al. (KLOE-2), Phys. Lett. **B706**, 251 (2012), 1110.0411.
[38] D. Babusci et al. (KLOE-2), Phys. Lett. **B720**, 111 (2013), 1210.3927.
[39] D. Babusci et al. (KLOE-2), Phys. Lett. **B736**, 459 (2014), 1404.7772.
[40] A. Anastasi et al. (KLOE-2), Phys. Lett. **B757**, 356 (2016), 1603.06086.
[41] A. Anastasi et al. (KLOE-2), Phys. Lett. **B750**, 633 (2015), 1509.00740.
[42] A. Anastasi et al. (KLOE-2), Phys. Lett. **B747**, 365 (2015), 1501.06795.
[43] M. Anelli et al. (SHiP) (2015), 1504.04956.
[44] P. Ilten, Y. Soreq, J. Thaler, M. Williams, and W. Xue, Phys. Rev. Lett. **116**, 251803 (2016), 1603.08926.
[45] R. Aaij et al. (LHCb), Phys. Rev. Lett. **115**, 161802 (2015), 1508.04094.
[46] P. Ilten, J. Thaler, M. Williams, and W. Xue, Phys. Rev. **D92**, 115017 (2015), 1509.06765.
[47] J. L. Feng, Ann. Rev. Astron. Astrophys. **48**, 495 (2010), 1003.0904.
[48] P. deNiverville, M. Pospelov, and A. Ritz, Phys. Rev. **D84**, 075020 (2011), 1107.4580.
[49] Y. Kahn, G. Krnjaic, J. Thaler, and M. Toups (2014), 1411.1055.
[50] L. B. Auerbach et al. (LSND), Phys. Rev. **D63**, 112001 (2001), hep-ex/0101039.
[51] B. Batell, R. Essig, and Z. Surujon, Phys. Rev. Lett. **113**, 171802 (2014), 1406.2698.
[52] J. D. Bjorken, S. Ecklund, W. R. Nelson, A. Abashian, C. Church, B. Lu, L. W. Mo, T. A. Nunamaker, and P. Rassmann, Phys. Rev. **D38**, 3375 (1988).
[53] M. S. Atiya, I.-H. Chiang, J. S. Frank, J. S. Haggerty, M. M. Ito, T. F. Kycia, K. K. Li, L. S. Littenberg, A. J. Stevens, A. Sambamurti, et al., Phys. Rev. Lett. **69**, 733 (1992), URL `http://link.aps.org/doi/10.1103/PhysRevLett.69.733`.
[54] A. V. Artamonov et al. (BNL-E949), Phys. Rev. **D79**, 092004 (2009), 0903.0030.
[55] M. Ablikim et al. (BES), Phys. Rev. Lett. **100**, 192001 (2008), 0710.0039.
[56] B. Aubert et al. (BaBar), in *Proceedings, 34th International Conference on High Energy Physics (ICHEP 2008)* (2008), 0808.0017, URL `http://www-public.slac.stanford.edu/sciDoc/docMeta.aspx?slacPubNumber=slac-pub-13328`.
[57] R. Essig, J. Mardon, M. Papucci, T. Volansky, and Y.-M. Zhong, JHEP **11**, 167 (2013), 1309.5084.
[58] I. M. Shoemaker and L. Vecchi, Phys. Rev. **D86**, 015023 (2012), 1112.5457.
[59] H. An, X. Ji, and L.-T. Wang, JHEP **07**, 182 (2012), 1202.2894.
[60] R. Bouchendira, P. Clade, S. Guellati-Khelifa, F. Nez, and F. Biraben, Phys. Rev. Lett. **106**, 080801 (2011), 1012.3627.
[61] T. Aoyama, M. Hayakawa, T. Kinoshita, and M. Nio, Phys. Rev. Lett. **109**, 111807 (2012), 1205.5368.
[62] D. Hanneke, S. F. Hoogerheide, and G. Gabrielse, Phys. Rev. **A83**, 052122 (2011), 1009.4831.
[63] B. Batell, M. Pospelov, and A. Ritz, Phys. Rev. **D80**, 095024 (2009), 0906.5614.
[64] P. deNiverville, D. McKeen, and A. Ritz, Phys. Rev. **D86**, 035022 (2012), 1205.3499.
[65] R. Dharmapalan et al. (MiniBooNE) (2012), 1211.2258.
[66] B. Batell, P. deNiverville, D. McKeen, M. Pospelov, and A. Ritz (2014), 1405.7049.
[67] D. Gorbunov, A. Makarov, and I. Timiryasov, Phys. Rev. **D91**, 035027 (2015), 1411.4007.
[68] J. Blümlein and J. Brunner, Phys. Lett. **B731**, 320 (2014), 1311.3870.
[69] K. Abe et al. (T2K), Phys. Rev. **D90**, 072012 (2014), 1403.3140.

[70] P. Coloma, B. A. Dobrescu, C. Frugiuele, and R. Harnik, JHEP **04**, 047 (2016), 1512.03852.
[71] S. Alekhin et al. (2015), 1504.04855.
[72] E. Izaguirre, G. Krnjaic, P. Schuster, and N. Toro, Phys. Rev. **D88**, 114015 (2013), 1307.6554.
[73] M. Battaglieri et al. (BDX) (2014), 1406.3028.
[74] J. Alexander (2016), URL `https://indico.cern.ch/event/507783/contributions/2150181/attachments/1266367/1874844/SLAC-MMAPS-alexander.pdf`.
[75] G. F. Giudice, P. Paradisi, and M. Passera, JHEP **11**, 113 (2012), 1208.6583.
[76] B. Aubert et al. (BaBar), in *Proceedings, 34th International Conference on High Energy Physics (ICHEP 2008): Philadelphia, Pennsylvania, July 30-August 5, 2008* (2008), 0808.0017, URL `http://www-public.slac.stanford.edu/sciDoc/docMeta.aspx?slacPubNumber=slac-pub-13328`.
[77] S. Adler et al. (E787 Collaboration), Phys.Rev. **D70**, 037102 (2004), hep-ex/0403034.
[78] E. Izaguirre, G. Krnjaic, P. Schuster, and N. Toro, Phys. Rev. **D91**, 094026 (2015), 1411.1404.
[79] E. Izaguirre, G. Krnjaic, P. Schuster, and N. Toro, Phys. Rev. Lett. **115**, 251301 (2015), 1505.00011.
[80] R. Essig, J. Mardon, M. Papucci, T. Volansky, and Y.-M. Zhong, JHEP **11**, 167 (2013), 1309.5084.
[81] J. Abdallah et al., Phys. Dark Univ. **9-10**, 8 (2015), 1506.03116.
[82] Y. Bai and T. M. P. Tait, Phys. Lett. **B710**, 335 (2012), 1109.4144.
[83] N. Weiner and I. Yavin, Phys. Rev. **D86**, 075021 (2012), 1206.2910.
[84] M. Autran, K. Bauer, T. Lin, and D. Whiteson, Phys. Rev. **D92**, 035007 (2015), 1504.01386.
[85] Y. Bai, J. Bourbeau, and T. Lin, JHEP **06**, 205 (2015), 1504.01395.
[86] B. A. Dobrescu and C. Frugiuele, Phys. Rev. Lett. **113**, 061801 (2014), 1404.3947.
[87] E. Izaguirre, G. Krnjaic, P. Schuster, and N. Toro, Phys. Rev. **D90**, 014052 (2014), 1403.6826.
[88] M. W. Goodman and E. Witten, Phys.Rev. **D31**, 3059 (1985).
[89] P. Cushman et al., in *Community Summer Study 2013: Snowmass on the Mississippi (CSS2013) Minneapolis, MN, USA, July 29-August 6, 2013* (2013), 1310.8327, URL `http://arxiv.org/pdf/1310.8327.pdf`.
[90] G. Angloher et al. (CRESST), Eur. Phys. J. **C76**, 25 (2016), 1509.01515.
[91] R. Essig, A. Manalaysay, J. Mardon, P. Sorensen, and T. Volansky, Phys. Rev. Lett. **109**, 021301 (2012), 1206.2644.
[92] J. Angle et al. (XENON10 Collaboration), Phys.Rev.Lett. **107**, 051301 (2011), 1104.3088.
[93] P. W. Graham, D. E. Kaplan, S. Rajendran, and M. T. Walters, Phys. Dark Univ. **1**, 32 (2012), 1203.2531.
[94] S. K. Lee, M. Lisanti, S. Mishra-Sharma, and B. R. Safdi, Phys. Rev. **D92**, 083517 (2015), 1508.07361.
[95] R. Essig, M. Fernandez-Serra, J. Mardon, A. Soto, T. Volansky, and T.-T. Yu (2015), 1509.01598.
[96] J. Barreto et al. (DAMIC Collaboration), Phys.Lett. **B711**, 264 (2012), 1105.5191.
[97] S. Derenzo, R. Essig, A. Massari, A. Soto, and T.-T. Yu (2016), 1607.01009.
[98] Y. Hochberg, Y. Kahn, M. Lisanti, C. G. Tully, and K. M. Zurek (2016), 1606.08849.
[99] Y. Hochberg, Y. Zhao, and K. M. Zurek, Phys. Rev. Lett. **116**, 011301 (2016), 1504.07237.
[100] Y. Hochberg, M. Pyle, Y. Zhao, and K. M. Zurek (2015), 1512.04533.
[101] K. Schutz and K. M. Zurek (2016), 1604.08206.
[102] D. S. Akerib et al. (LUX), Phys. Rev. Lett. **116**, 161301 (2016), 1512.03506.
[103] G. Angloher and Others (CRESST), The European Physical Journal C **76**, 1 (2016), ISSN

1434-6052, URL http://dx.doi.org/10.1140/epjc/s10052-016-3877-3.
[104] R. Agnese and others (SuperCDMS Soudan) (SuperCDMS Collaboration), Phys. Rev. Lett. **116**, 071301 (2016), URL http://link.aps.org/doi/10.1103/PhysRevLett.116.071301.
[105] A. K. Drukier, K. Freese, and D. N. Spergel, Phys. Rev. **D33**, 3495 (1986).
[106] T. Lin, H.-B. Yu, and K. M. Zurek, Phys. Rev. **D85**, 063503 (2012), 1111.0293.
[107] H. An, M. Pospelov, and J. Pradler, Phys.Rev.Lett. **111**, 041302 (2013), 1304.3461.
[108] Y. Hochberg, T. Lin, and K. M. Zurek (2016), 1604.06800.
[109] N. Arkani-Hamed, D. P. Finkbeiner, T. R. Slatyer, and N. Weiner, Phys. Rev. **D79**, 015014 (2009), 0810.0713.
[110] M. Pospelov and A. Ritz, Phys. Lett. **B671**, 391 (2009), 0810.1502.
[111] J. D. Bjorken, R. Essig, P. Schuster, and N. Toro, Phys. Rev. **D80**, 075018 (2009), 0906.0580.
[112] B. Batell, M. Pospelov, and A. Ritz, Phys. Rev. **D79**, 115008 (2009), 0903.0363.
[113] R. Essig, P. Schuster, and N. Toro, Phys. Rev. **D80**, 015003 (2009), 0903.3941.
[114] J. P. Lees et al. (BABAR), Phys. Rev. Lett. **108**, 211801 (2012), 1202.1313.
[115] J. D. Clarke, R. Foot, and R. R. Volkas, JHEP **02**, 123 (2014), 1310.8042.
[116] N. Arkani-Hamed and N. Weiner, JHEP **12**, 104 (2008), 0810.0714.
[117] C. Cheung, J. T. Ruderman, L.-T. Wang, and I. Yavin, Phys. Rev. **D80**, 035008 (2009), 0902.3246.
[118] D. E. Morrissey, D. Poland, and K. M. Zurek, JHEP **07**, 050 (2009), 0904.2567.
[119] G. Aad et al. (ATLAS), JHEP **11**, 088 (2014), 1409.0746.
[120] V. Khachatryan et al. (CMS), Phys. Lett. **B752**, 146 (2016), 1506.00424.
[121] G. Barello, S. Chang, and C. A. Newby (2015), 1511.02865.
[122] D. S. M. Alves, S. R. Behbahani, P. Schuster, and J. G. Wacker, Phys. Lett. **B692**, 323 (2010), 0903.3945.
[123] K. Harigaya and Y. Nomura (2016), 1603.03430.
[124] M. J. Strassler and K. M. Zurek, Phys. Lett. **B651**, 374 (2007), hep-ph/0604261.
[125] T. Han, Z. Si, K. M. Zurek, and M. J. Strassler, JHEP **07**, 008 (2008), 0712.2041.
[126] P. Schwaller, D. Stolarski, and A. Weiler, JHEP **05**, 059 (2015), 1502.05409.
[127] T. Cohen, M. Lisanti, and H. K. Lou, Phys. Rev. Lett. **115**, 171804 (2015), 1503.00009.
[128] P. A. R. Ade et al. (Planck) (2015), 1502.01589.
[129] B. Moore, Nature **370**, 629 (1994).
[130] R. A. Flores and J. R. Primack, Astrophys. J. **427**, L1 (1994), astro-ph/9402004.
[131] M. Boylan-Kolchin, J. S. Bullock, and M. Kaplinghat, Mon. Not. Roy. Astron. Soc. **415**, L40 (2011), 1103.0007.
[132] F. Governato, A. Zolotov, A. Pontzen, C. Christensen, S. H. Oh, A. M. Brooks, T. Quinn, S. Shen, and J. Wadsley, Mon. Not. Roy. Astron. Soc. **422**, 1231 (2012), 1202.0554.
[133] J. Onorbe, M. Boylan-Kolchin, J. S. Bullock, P. F. Hopkins, D. Keres, C.-A. Faucher-Giguere, E. Quataert, and N. Murray, Mon. Not. Roy. Astron. Soc. **454**, 2092 (2015), 1502.02036.
[134] K. A. Oman et al., Mon. Not. Roy. Astron. Soc. **452**, 3650 (2015), 1504.01437.
[135] E. Papastergis and F. Shankar, ArXiv e-prints (2015), 1511.08741.
[136] D. N. Spergel and P. J. Steinhardt, Phys. Rev. Lett. **84**, 3760 (2000), astro-ph/9909386.
[137] M. Rocha, A. H. G. Peter, J. S. Bullock, M. Kaplinghat, S. Garrison-Kimmel, J. Onorbe, and L. A. Moustakas, Mon. Not. Roy. Astron. Soc. **430**, 81 (2013), 1208.3025.
[138] M. Vogelsberger, J. Zavala, and A. Loeb, Mon. Not. Roy. Astron. Soc. **423**, 3740 (2012), 1201.5892.
[139] S. W. Randall, M. Markevitch, D. Clowe, A. H. Gonzalez, and M. Bradac, Astrophys. J.

679, 1173 (2008), 0704.0261.
[140] M. R. Buckley and P. J. Fox, Phys. Rev. **D81**, 083522 (2010), 0911.3898.
[141] A. H. G. Peter, M. Rocha, J. S. Bullock, and M. Kaplinghat, Mon. Not. Roy. Astron. Soc. **430**, 105 (2013), 1208.3026.
[142] S. Tulin, H.-B. Yu, and K. M. Zurek, Phys. Rev. **D87**, 115007 (2013), 1302.3898.
[143] M. Kaplinghat, S. Tulin, and H.-B. Yu, Phys. Rev. Lett. **116**, 041302 (2016), 1508.03339.
[144] A. Fradette, M. Pospelov, J. Pradler, and A. Ritz, Phys. Rev. **D90**, 035022 (2014), 1407.0993.
[145] J. Berger, K. Jedamzik, and D. G. E. Walker (2016), 1605.07195.
[146] J. L. Feng, M. Kaplinghat, H. Tu, and H.-B. Yu, JCAP **0907**, 004 (2009), 0905.3039.
[147] D. E. Kaplan, G. Z. Krnjaic, K. R. Rehermann, and C. M. Wells, JCAP **1005**, 021 (2010), 0909.0753.
[148] H. An, B. Echenard, M. Pospelov, and Y. Zhang, Phys. Rev. Lett. **116**, 151801 (2016), 1510.05020.
[149] H. An, M. B. Wise, and Y. Zhang (2016), 1604.01776.
[150] Y. Tsai, L.-T. Wang, and Y. Zhao, Phys. Rev. **D93**, 035024 (2016), 1511.07433.
[151] E. D. Carlson, M. E. Machacek, and L. J. Hall, Astrophys. J. **398**, 43 (1992).
[152] Y. Hochberg, E. Kuflik, T. Volansky, and J. G. Wacker, Phys. Rev. Lett. **113**, 171301 (2014), 1402.5143.
[153] E. Kuflik, M. Perelstein, N. R.-L. Lorier, and Y.-D. Tsai (2015), 1512.04545.
[154] G. Gelmini, P. Gondolo, A. Soldatenko, and C. E. Yaguna, Phys. Rev. **D74**, 083514 (2006), hep-ph/0605016.
[155] D. E. Kaplan, M. A. Luty, and K. M. Zurek, Phys. Rev. **D79**, 115016 (2009), 0901.4117.
[156] H. Davoudiasl, D. E. Morrissey, K. Sigurdson, and S. Tulin, Phys. Rev. **D84**, 096008 (2011), 1106.4320.
[157] T. Blum, A. Denig, I. Logashenko, E. de Rafael, B. Lee Roberts, T. Teubner, and G. Venanzoni (2013), 1311.2198.
[158] R. Pohl et al., Nature **466**, 213 (2010).
[159] A. Krasznahorkay et al., Phys. Rev. Lett. **116**, 042501 (2016), 1504.01527.
[160] J. Heeck, Phys. Lett. **B739**, 256 (2014), 1408.6845.
[161] W. Altmannshofer, S. Gori, M. Pospelov, and I. Yavin, Phys. Rev. **D89**, 095033 (2014), 1403.1269.
[162] C.-Y. Chen, H. Davoudiasl, W. J. Marciano, and C. Zhang, Phys. Rev. **D93**, 035006 (2016), 1511.04715.
[163] B. Batell, N. Lange, D. McKeen, M. Pospelov, and A. Ritz (2016), 1606.04943.
[164] J. L. Feng, B. Fornal, I. Galon, S. Gardner, J. Smolinsky, T. M. P. Tait, and P. Tanedo (2016), 1604.07411.
[165] S. Gardner, R. J. Holt, and A. S. Tadepalli (2015), 1509.00050.
[166] A. Haas, C. S. Hill, E. Izaguirre, and I. Yavin, Phys. Lett. **B746**, 117 (2015), 1410.6816.
[167] P. Schuster, N. Toro, and I. Yavin, Phys. Rev. **D81**, 016002 (2010), 0910.1602.
[168] K. Agashe, Y. Cui, L. Necib, and J. Thaler, JCAP **1410**, 062 (2014), 1405.7370.
[169] J. Berger, Y. Cui, and Y. Zhao, JCAP **1502**, 005 (2015), 1410.2246.
[170] G. Aad et al. (ATLAS), JHEP **04**, 169 (2014), 1402.7029.
[171] S. Chatrchyan et al. (CMS), Phys. Rev. **D90**, 032006 (2014), 1404.5801.
[172] M. Backovic, K. Kong, and M. McCaskey, Physics of the Dark Universe **5-6**, 18 (2014), 1308.4955.
[173] M. Backović, A. Martini, O. Mattelaer, K. Kong, and G. Mohlabeng, Phys. Dark Univ. **9-10**,

37 (2015), 1505.04190.
[174] B. Aubert et al. (BABAR), in *Proceedings, 24th International Symposium on Lepton-Photon Interactions at High Energy (LP09)* (2009), 0908.2821, URL http://www-public.slac.stanford.edu/sciDoc/docMeta.aspx?slacPubNumber=SLAC-PUB-13758.
[175] (2016), 1606.03501.
[176] G. Aad et al. (ATLAS), JHEP **02**, 062 (2016), 1511.05542.
[177] G. Aad et al. (ATLAS), Phys. Rev. **D92**, 012010 (2015), 1504.03634.
[178] G. Aad et al. (ATLAS), Phys. Lett. **B743**, 15 (2015), 1501.04020.
[179] G. Aad et al. (ATLAS), Phys. Rev. **D92**, 052002 (2015), 1505.01609.
[180] G. Aad et al. (ATLAS), Phys. Rev. **D92**, 092001 (2015), 1505.07645.
[181] G. Aad et al. (ATLAS), Eur. Phys. J. **C76**, 210 (2016), 1509.05051.
[182] Tech. Rep. ATLAS-CONF-2015-001, CERN, Geneva (2015), URL https://cds.cern.ch/record/1988425.
[183] V. Khachatryan et al. (CMS), Phys. Rev. **D91**, 052012 (2015), 1411.6977.
[184] V. Khachatryan et al. (CMS), Phys. Rev. **D91**, 012007 (2015), 1411.6530.
[185] V. Khachatryan et al. (CMS), JHEP **01**, 079 (2016), 1510.06534.
[186] Tech. Rep. CMS-PAS-HIG-14-041, CERN, Geneva (2016), URL https://cds.cern.ch/record/2135985.
[187] Tech. Rep. CMS-PAS-HIG-15-011, CERN, Geneva (2016), URL https://cds.cern.ch/record/2128149.
[188] V. Khachatryan et al. (CMS), Phys. Lett. **B753**, 363 (2016), 1507.00359.
[189] R. Aaij et al. (LHCb), Eur. Phys. J. **C75**, 152 (2015), 1412.3021.
[190] R. Aaij et al. (LHCb), Phys. Rev. **D85**, 112004 (2012), 1201.5600.
[191] R. Aaij et al. (LHCb), Phys. Rev. Lett. **112**, 131802 (2014), 1401.5361.
[192] F. Bergsma et al. (CHARM), Phys. Lett. **B157**, 458 (1985).
[193] J. D. Bjorken, S. Ecklund, W. R. Nelson, A. Abashian, C. Church, B. Lu, L. W. Mo, T. A. Nunamaker, and P. Rassmann, Phys. Rev. **D38**, 3375 (1988).
[194] D. Geiregat et al. (CHARM-II), Phys. Lett. **B245**, 271 (1990).
[195] S. R. Mishra et al. (CCFR), Phys. Rev. Lett. **66**, 3117 (1991).
[196] W. Altmannshofer, S. Gori, M. Pospelov, and I. Yavin, Phys. Rev. Lett. **113**, 091801 (2014), 1406.2332.
[197] J. de Favereau, C. Delaere, P. Demin, A. Giammanco, V. Lemaître, A. Mertens, and M. Selvaggi (DELPHES 3), JHEP **02**, 057 (2014), 1307.6346.
[198] Since the energies of the experiments considered here are well below the electroweak scale, it is appropriate to only consider the $U(1)_{\rm em}$ gauge group of the SM. In a more fundamental theory above the weak scale, the kinetic mixing would involve the $U(1)_Y$ group instead; such a theory would always reduce to (11) below the weak scale.
[199] It is possible that dedicated downstream detectors may be sensitive to long-lived dark sector states produced in A' decays; this will be discussed in the Dark Matter at Accelerators section of this Report.
[200] Similar signatures arise in simplified models of inelastic DM [8, 13, 82].
[201] This is in the form both of published efficiency information, as well as cards for fast detector simulations such as `Delphes` [197] that are validated with experimental data.